DECLARATION OF GORDON MACPHERSON

I, Gordon MacPherson, am over twenty-one (21) years of age. I have never been convicted of a felony, and I am fully competent to make this declaration. I declare the following to be true to the best of my knowledge, information, and belief:

1. I am the Director, Board Governance & Policy Development at The Institute of Electrical and Electronics Engineers, Incorporated ("IEEE").
2. IEEE is a neutral third party in this dispute.
3. I am not being compensated for this declaration and IEEE is only being reimbursed for the cost of the article I am certifying.
4. Among my responsibilities as Director of Board Governance & Policy Development, I act as a custodian of certain records for IEEE.
5. I make this declaration based on my personal knowledge and information contained in the business records of IEEE.
6. As part of its ordinary course of business, IEEE publishes and makes available technical articles and standards. These publications are made available for public download through the IEEE digital library, IEEE Xplore.
7. It is the regular practice of IEEE to publish articles and other writings including article abstracts and make them available to the public through IEEE Xplore. IEEE maintains copies of publications in the ordinary course of its regularly conducted activities.
8. The articles below have been attached as Exhibit A-Exhibit C to this declaration:

Exhibit A	P. Ciais, R. Staraj, G. Kossiavas and C. Luxey, "Design of an Internal Quad-Band Antenna for Mobile Phones," in *IEEE Microwave and Wireless Components Letters*, vol. 14, no. 4, pp. 148-150, May 2004, doi: 10.1109/LMWC.2004.825186
Exhibit B	H. Nakano, Y. Sato, H. Mimaki and J. Yamauchi, "An Inverted FL Antenna for Dual-Frequency Operation," in *IEEE Transactions on Antennas and Propagation*, vol. 53, no. 8, pp. 2417-2421, Aug. 2005, doi: 10.1109/TAP.2005.852502
Exhibit C	Xu Jing, Zhengwei Du and Ke Gong, "Compact Planar Monopole Antenna for Multi-Band Mobile Phones," *2005 Asia-Pacific Microwave Conference Proceedings*, Suzhou, 2005, doi: 10.1109/APMC.2005.1606884

9. I obtained a copy of Exhibit A through IEEE Xplore, where it is maintained in the ordinary course of IEEE's business. Exhibit A is a true and correct copy of the Exhibit, as it existed on or about May 5, 2025.

10. I obtained a copy of Exhibit B through IEEE Xplore, where it is maintained in the ordinary course of IEEE's business. Exhibit B is a true and correct copy of the Exhibit, as it existed on or about May 5, 2025.

11. I obtained a copy of Exhibit C through IEEE Xplore, where it is maintained in the ordinary course of IEEE's business. Exhibit C is a true and correct copy of the Exhibit, as it existed on or about May 5, 2025.

12. The articles and abstracts from IEEE Xplore show the dates of publication. IEEE Xplore populates this information using the metadata associated with the publication.

13. P. Ciais, R. Staraj, G. Kossiavas and C. Luxey, "Design of an Internal Quad-Band Antenna for Mobile Phones," was published in *IEEE Microwave and Wireless Components Letters Journal* (Vol. 14, No. 4, pages. 148-150, date of publication May 4, 2004). This article is currently available for public download from the IEEE digital library, IEEE Xplore.

14. H. Nakano, Y. Sato, H. Mimaki and J. Yamauchi, "An Inverted FL Antenna for Dual-Frequency Operation," was published in *IEEE Transactions on Antennas and Propagation Journal (*Vol. 53, No. 8, pages 2417-2421, date of publication August 2005). This article is currently available for public download from the IEEE digital library, IEEE Xplore.

15. Xu Jing, Zhengwei Du and Ke Gong, "Compact Planar Monopole Antenna for Multi-Band Mobile Phones," was published in *2005 Asia-Pacific Microwave Conference Proceedings*, held in Suzhou, China on December 04-07, 2005. Copies of the conference proceeding were made available no later than the last day of conference. This article currently available for public download from IEEE digital library, IEEE Xplore.

I hereby declare that all statements made herein of my own knowledge are true and that all statements made on information and belief are believed to be true, and further that these statements were made with the knowledge that willful false statements and the like are punishable by fine or imprisonment, or both, under 18 U.S.C. § 1001.

I declare under penalty of perjury that the foregoing statements are true and correct.

Date: 5/6/2025

By: Signed by: Gordon MacPherson 845214E4A5C0470...

EXHIBIT A

Design of an Internal Quad-Band Antenna for Mobile Phones

Pascal Ciais, Robert Staraj, Georges Kossiavas, and Cyril Luxey

***Abstract*—This letter presents the design of a compact Planar Inverted-F Antenna (PIFA) suitable for cellular telephone applications. The quarter-wavelength antenna combines the use of a slot, shorted parasitic patches and capacitive loads to achieve multiband operation. The commercial electromagnetic software IE3D is used to design and optimize the structure. The resulting antenna can operate from 880 to 960 MHz and 1710 to 2170 MHz covering GSM, DCS, PCS, and UMTS standards with a VSWR better than 2.5. Good agreement is found between simulated and measured results.**

***Index Terms*—Handset antennas, multiband antennas, planar inverted-F antennas (PIFAs), small antennas.**

I. Introduction

With the rapid progress in new communication standards, miniature multiband internal antennas are needed for modern mobile handsets [1]–[3]. Several techniques applied simultaneously are thus necessary to reduce the size of these antennas while maintaining good multiband/wideband performance.

The antenna presented in this letter combines several of these techniques. The main resonator is a dual-band PIFA antenna tuned to operate at center frequencies of 935 MHz and 1930 MHz. The introduction of a slot into this element allows a frequency decrease of its fundamental resonance while the use of an end positioned capacitive load allows its higher order modes to be decreased in frequency (Fig. 1) [4]. Instead of the previously reported tunable scheme [2], the addition of three quarter-wavelength parasitic elements is used here to create new resonances [5]–[7] and thus enlarge both lower and upper impedance bandwidth. These new resonances are tuned thanks to a lengthening by capacitive loads [7]. This antenna covers the GSM standard (Global System for Mobile communications, 880–960 MHz) with a VSWR (Voltage Standing Wave Ratio) better than 2.5 and also the DCS (Digital Communication System, 1710–1880 MHz), PCS (Personal Communication Services, 1850–1990 MHz) and UMTS (Universal Mobile Telecommunications System, 1920–2170 MHz) standards with a VSWR less than 2.

II. Antenna Structure and Design Rules

The antenna consists of a main patch with three additional parasitic elements placed on the corner of a ground plane

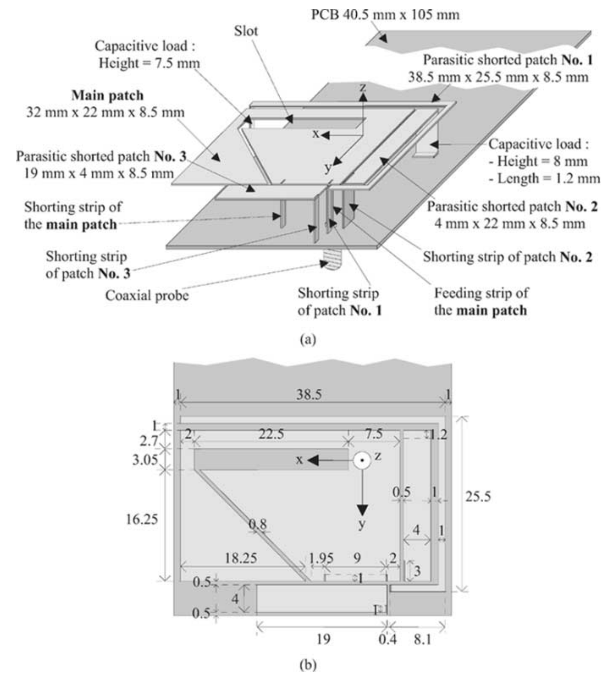

Fig. 1. Configuration of the quad-band antenna. (a) Side view. (b) Top view : all dimensions are in millimeter.

whose size is representative of the Printed Circuit Board (PCB) of a typical mobile phone: 40.5 mm $\times$ 105 mm (Fig. 1). The PCB size, especially its length, has a strong influence on the performances of mobile phone antennas. In our case, the chosen length is not the best choice for an optimum GSM bandwidth (around 130 mm [9]–[11]) or an optimum DCS bandwidth (around 70 mm [9]–[11]) but it will equally helps in these both bands for an efficient antenna-chassis combination. The dielectric between all patches and the PCB is air and the separation distance is 8.5 mm.

The main quarter-wavelength patch is coaxially fed via a metallic strip. The first objective is to get a proper resonance in the GSM band, where the approximate formula: $f_r = c/4(L+H)$, is used as a starting rule for the design of the patch (with $f_r =$ resonant frequency of the patch, $c =$ velocity of light in free space, $L =$ average length of the patch, and $H =$ height of the patch). The analytical length of a 8.5 mm height quarter-wavelength resonator is then found to be 71.7 mm at 935 MHz in the GSM band. This length can be slightly reduced by using a partial shorting strip instead of a plain shorting wall. Moreover, it has been previously shown that both the antenna with its feeding and shorting pins always have to be positioned at the top of the PCB to obtain an efficient

Manuscript received July 17, 2003; revised November 21, 2003. This work was supported by France Telecom R&D under Contract 424 76-344.

The authors are with the Laboratoire d'Electronique, Antennes et Télécommunications, Université de Nice-Sophia Antipolis/UMR-CNRS 6071, 06560 Valbonne, France (e-mail: ciaisp@elec.unice.fr).

Digital Object Identifier 10.1109/LMWC.2004.825186

antenna-chassis combination, especially maximum bandwidth behavior [8]–[11]. In such a configuration, the matching of the antenna to a 50 Ω source is not so difficult to achieve since the 50 Ω input impedance point is not spatially far from the shorting strip. However, due to its intrinsic properties, the design at 935 MHz of a rectangular quarter-wavelength patch with its length aligned with the PCB length, will only lead to an odd number of higher resonance frequencies namely 2805 MHz (3 f_r), 4675 MHz (5 f_r), and so on. As our main element need to resonate in the 1710–2170 MHz band, we need to decrease the working frequency of the 3rd higher mode of this structure. It has been successfully demonstrated in [9] that adding a capacitive load to the structure will result in a decrease of the frequency of its higher modes. This can be achieved by folding the patch over on itself. The value of this capacitance can be controlled by increasing or decreasing the metal facing surfaces. However, this folding operation also reduces the bandwidth of the antenna due to an inherent increase of its total quality factor Q [12].

Three parasitic elements have to be added to the main patch to achieve our desired multiband goal. These elements are chosen quarter-wavelength type, each connected to the ground plane by metallic strips and located near the main patch in order to be correctly electromagnetically excited. Capacitive loads can be added to these parasitic patches by vertically folding their strip ends. Hence, the electrical lengths of these resonators are artificially increased without enlarging the whole antenna size. A first parasitic patch have to be added to enlarge the GSM bandwidth (no. 1 on Fig. 1), its theoretical quarter-wavelength is found to be 76 mm at 888 MHz. Two others parasitic patches must be added to increase the upper bandwidth (no. 2 and no. 3 on Fig. 1). Their theoretical lengths are 34.1 mm at 1760 MHz and 26.9 mm at 2120 MHz.

III. Results

With these empirical design rules, a dual-band patch antenna was first designed and optimized using a simulation tool based on the method of moments : IE3D [13]. Parasitic patches no. 2 and no. 3 were then separately and simultaneously added to this main patch. At last, parasitic patch no. 1 was built to achieve the final goal. All structures have been fine tuned to achieve the best possible coupling between the resonances i.e the largest possible bandwidths. This tuning was made by slightly changing the main dimensions of the parasitic patches and/or their gaps with the main patch. All the optimized dimensions of each stage are not listed here for brevity. Fig. 2 shows the simulated VSWR of the main patch with and without parasitic shorted patches no. 2 and no. 3. It is seen on this graph that the main patch alone has two resonances in the GSM band and around 2 GHz with both small bandwidths. The VSWR curves of the main patch with the addition of only one parasitic patch (no. 2 or no. 3) are also plotted on this graph. In both cases, it increases the upper bandwidth of the first antenna in two different ways: parasitic no. 2 works below the 3rd resonance of the main patch while parasitic No. 3 works above. The simulated VSWR of the main plate with the simultaneous addition of these two shorted patches is also plotted on Fig. 2. This structure has now an upper bandwidth of 470 MHz (1705–2175 MHz)

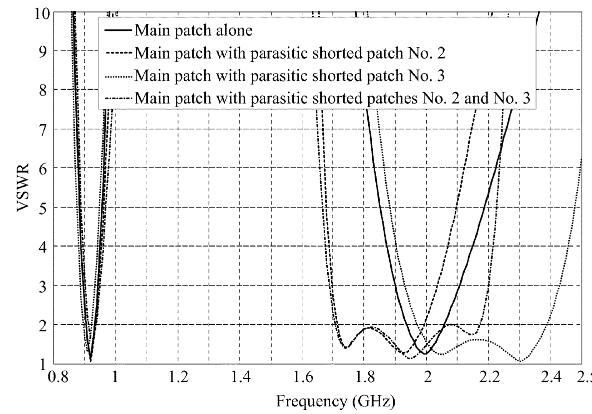

Fig. 2. Simulated VSWR of the main patch with and without parasitic shorted patches no. 2 and no. 3.

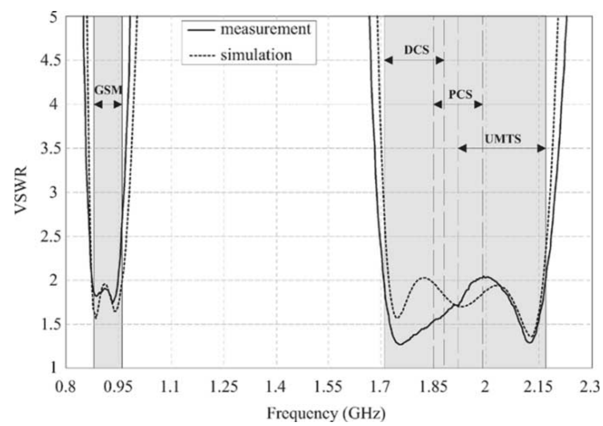

Fig. 3. Measured and simulated VSWR of the quad-band antenna.

with a VSWR less than 2 covering the DCS, PCS and UMTS standards but the lower bandwidth of 40 MHz (905–945 MHz) with a VSWR less than 2.5 is clearly insufficient to cover the entire GSM band. The performances of the main antenna with parasitics no. 2 and no. 3 shows that an additional parasitic element no. 1 is needed to increase the low part of the GSM band. Fig. 3 compares the simulated and measured VSWR of the final quad-band antenna (dimensions 38.5 mm × 28.5 mm × 8.5 mm). The step by step optimization of the structure resulted in a folded dual-band patch antenna of dimensions 32 mm × 22 mm × 8.5 mm with a strong quasilocalized capacitive load at its end and an average quarter-wavelength length of 72.2 mm that is very close to the theoretical value of 71.7 mm. The physical length of parasitic patch no. 1 is 77.6 mm, compared with the theoretical quarter-wavelength of 76 mm at 888 MHz. Capacitive loads were added to the parasitic patches no. 1 and no. 2 by vertically folding their strip ends. Physical lengths of elements no. 2 and no. 3 are respectively 31.2 mm and 19 mm to be compared with the theoretical quarter-wavelengths of 34.1 mm at 1760 MHz and 26.9 mm at 2120 MHz. The small discrepancies between these values comes from the theoretical formula which doesn't take into account localized and distributed capacitive loading effects. This capacitive effect is very strong in the case of parasitic element no. 3 where two high impedance portions of metal face each others. A good agreement between theoretical and experimental results is observed. The measured lower bandwidth is 90 MHz (870–960 MHz) with

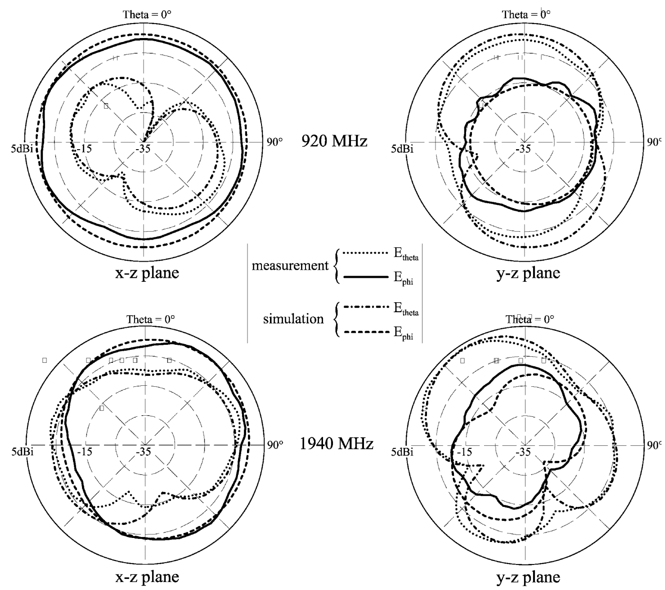

Fig. 4. Measured and simulated radiation gain patterns at 920 MHz and 1940 MHz for the quad-band antenna. Antenna orientation is given in Fig. 1.

a VSWR better than 2.5 while the upper bandwidth is 460 MHz (1710–2170 MHz) with a VSWR less than 2.

The measured and simulated radiation gain patterns of the antenna at 920 MHz and 1940 MHz are depicted in Fig. 4. These patterns reveal a quasi omnidirectional character in the x-z plane as well as a lack of polarization purity due to the radiation from the PCB. However, these two properties are not a drawback in mobile phone applications where omnidirectional radiation patterns as well as both vertical and horizontal electromagnetic field polarization occur in urban environments [14]. These omnidirectional patterns are due to the dipole-like behavior of the structure coming from the antenna-chassis combination : due to the in-phase currents flowing on the PCB in the GSM band, quasi perfect omnidirectional pattern is seen while some directivity appears at 1940 MHz in both planes since the length of the PCB is now larger than half the wavelength. Some discrepancies are found between theoretical and experimental far-field patterns. The small ripple seen in the measured curves comes principally from our measurement setup, especially from the radiation contribution of the feed cable of the antenna : in small antenna measurements, it is difficult to correctly choke the feed cable to avoid currents flowing on it [15], [16]. The measured maximum gains for the antenna are 1 dBi at 920 MHz and 3.3 dBi at 1940 MHz while the simulated are respectively 1.3 dBi and 3.5 dBi. The small discrepancies between these values are mainly attributed to the dielectric losses of the plastic support used in our radiation pattern measurement setup to maintain the antenna.

The efficiency of the structure, defined as the total radiated power divided by the incident power at the feed, takes into account reflection losses due to the mismatch between the coaxial probe and the antenna as well as ohmic losses. The computed efficiency was respectively above 69% and 74% in the GSM and DCS/PCS/UMTS bands which is suitable for mobile phone communication terminals.

IV. Conclusion

A compact multiband PIFA antenna with parasitic elements was designed and placed on a realistic PCB ground plane. This new structure uses various techniques of miniaturization to achieve low return loss in both GSM and DCS/PCS/UMTS bands. The quasi omnidirectional gain radiation pattern characteristics with good efficiency over the covered frequency bands make this antenna suitable for mobile phone applications. Further work will be concentrated on the coverage of new 2.4 GHz and 5.2 GHz standards.

Acknowledgment

The authors would like to thank Prof. V. F. Fusco from the Queen's University of Belfast, Patrice Brachat from France Telecom R&D, and J. Baro for their fruitful remarks about this work.

References

[1] Y.-X. Guo, M. Y. W. Chia, and Z. N. Chen, "Miniature built-in quad band antennas for mobile handsets," *IEEE Antennas Wireless Propagat. Lett.*, vol. 2, pp. 30–32, 2003.

[2] N. C. Karmakar, P. Hendro, and L. S. Firmansyah, "Shorting strap tunable single feed dual-band PIFA," *IEEE Microwave Wireless Comp. Lett.*, vol. 13, pp. 13–15, Jan. 2003.

[3] I. Ang, Y.-X. Guo, and Y. W. Chia, "Compact internal quad-band antenna for mobile phones," *Microw. Opt. Technol. Lett.*, vol. 38, no. 3, pp. 217–223, Aug. 2003.

[4] P. Salonen, M. Keskilammi, and M. Kivikoski, "New slot configurations for dual-band planar inverted-F antenna," *Microw. Opt. Technol. Lett.*, vol. 28, no. 5, pp. 293–298, Mar. 2001.

[5] Y. J. Wang, C. K. Lee, W. J. Koh, and Y. B. Gan, "Design of small and broad-band internal antennas for IMT-2000 mobile handsets," *IEEE Trans. Microw. Theory Tech.*, vol. 49, no. 8, pp. 1398–1403, Aug. 2001.

[6] C. T. P. Song, P. S. Hall, H. Ghafouri-Shiraz, and D. Wake, "Triple band planar inverted F antennas for handheld devices," *Electron. Lett.*, vol. 36, no. 2, pp. 112–114, Jan. 2000.

[7] J. Ollikainen, O. Kivekäs, A. Toropainen, and P. Vainikainen, "Internal dual-band patch antenna for mobile phones," in *Proc. Millennium Conf. Antennas Propagat.*, Davos, Switzerland, Apr. 2000, SP-444, session 3A9.

[8] M. Geissler, D. Heberling, and I. Wolff, "Properties of integrated handset antennas," in *Proc. Millenium Conf. Antennas Propagat.*, Davos, Switzerland, Apr. 2000, SP-444, session 5A5.

[9] D. Manteuffel, A. Bahr, D. Heberling, and I. Wolff, "Design considerations for integrated mobile phone antennas," in *Proc. 11th Int. Conf. Antennas Propagat.*, Apr. 2001, pp. 252–256.

[10] O. Kivekäs, J. Ollikainen, T. Lehtiemi, and P. Vainikainen, "Effect of the chassis length on the bandwidth, SAR, and efficiency of internal mobile phone antennas," *Microw. Opt. Technol. Lett.*, vol. 36, no. 6, pp. 457–462, Mar. 2003.

[11] P. Vainikainen, J. Ollikainen, O. Kivekäs, and I. Kelander, "Resonator-based analysis of the combination of mobile handset antenna and chassis," *IEEE Trans. Antennas Propagat.*, vol. 50, pp. 1433–1444, Oct. 2002.

[12] C. R. Rowell and R. D. Murch, "A capacitively loaded PIFA for compact mobile telephone handsets," *IEEE Trans. Antennas Propagat.*, vol. 45, pp. 837–842, May 1997.

[13] *IE3D, Release 9.33*, Zeland Software, Inc., 2002.

[14] K. Sulonen and P. Vainikainen, "Handset antenna evaluation based on measured distributions," in *Proc. IEEE Instrumentation and Measurement Technology Conf.*, Budapest, Hungary, May. 2001, pp. 519–524.

[15] J. Haley, T. Moore, and J. T. Bernhard, "Experimental investigation of antenna-handset-feed interaction during wireless product testing," *Microw. Opt. Technol. Lett.*, vol. 34, no. 3, pp. 169–172, Aug. 2002.

[16] C. Ilchen, J. Ollikainen, and P. Vainikainen, "Reducing the influence of feed cables on small antenna measurements," *Electron. Lett.*, vol. 35, no. 15, pp. 1212–1214, July 1999.

EXHIBIT A

ABSTRACT

Design of an internal quad-band antenna for mobile phones

Publisher: IEEE Cite This PDF

P. Ciais ; R. Staraj ; G. Kossiavas ; C. Luxey All Authors

Abstract:
This letter presents the design of a compact Planar Inverted-F Antenna (PIFA) suitable for cellular telephone applications. The quarter-wavelength antenna combines the use of a slot, shorted parasitic patches and capacitive loads to achieve multiband operation. The commercial electromagnetic software IE3D is used to design and optimize the structure. The resulting antenna can operate from 880 to 960 MHz and 1710 to 2170 MHz covering GSM, DCS, PCS, and UMTS standards with a VSWR better than 2.5. Good agreement is found between simulated and measured results.

Published in: IEEE Microwave and Wireless Components Letters (Volume: 14 , Issue: 4, April 2004)

Page(s): 148 - 150

DOI: 10.1109/LMWC.2004.825186

Date of Publication: 04 May 2004

Publisher: IEEE

ISSN Information:

SECTION I. Introduction

With the rapid progress in new communication standards, miniature multiband internal antennas are needed for modern mobile handsets [1]– [3]. Several techniques applied simultaneously are thus necessary to reduce the size of these antennas while maintaining good multiband/wideband performance.

The antenna presented in this letter combines several of these techniques. The main resonator is a dual-band PIFA antenna tuned to operate at center frequencies of 935 MHz and 1930 MHz. The introduction of a slot into this element allows a frequency decrease of its fundamental resonance while the use of an end positioned capacitive load allows its higher order modes to be decreased in frequency (Fig. 1) [4]. Instead of the previously reported tunable scheme [2], the addition of three quarter-wavelength parasitic elements is used here to create new resonances [5] [6] [7] and thus enlarge both lower and upper impedance bandwidth. These new resonances are tuned thanks to a lengthening by capacitive loads [7]. This antenna covers the GSM standard (Global System for Mobile communications, 880–960 MHz) with a VSWR (Voltage Standing Wave Ratio) better than 2.5 and also the DCS (Digital Communication System, 1710–1880 MHz), PCS (Personal Communication Services, 1850–1990 MHz) and UMTS (Universal Mobile Telecommunications System, 1920–2170 MHz) standards with a VSWR less than 2.

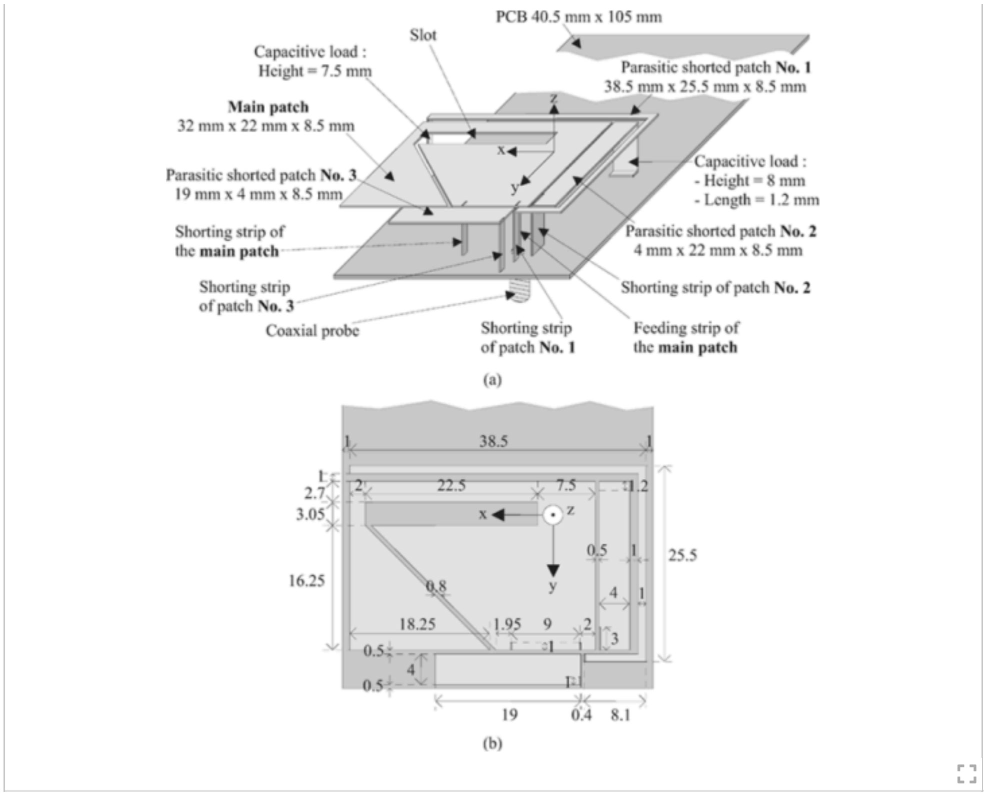

Fig. 1. Configuration of the quad-band antenna. (a) Side view. (b) Top view : all dimensions are in millimeter.

SECTION II.

Antenna Structure and Design Rules

The antenna consists of a main patch with three additional parasitic elements placed on the corner of a ground plane whose size is representative of the Printed Circuit Board (PCB) of a typical mobile phone: 40.5 mm×105 mm (Fig. 1). The PCB size, especially its length, has a strong influence on the performances of mobile phone antennas. In our case, the chosen length is not the best choice for an optimum GSM bandwidth (around 130 mm [9]– [11]) or an optimum DCS bandwidth (around 70 mm [9]– [11]) but it will equally helps in these both bands for an efficient antenna-chassis combination. The dielectric between all patches and the PCB is air and the separation distance is 8.5 mm.

The main quarter-wavelength patch is coaxially fed via a metallic strip. The first objective is to get a proper resonance in the GSM band, where the approximate formula: $f_r = c/4(L+H)$, is used as a starting rule for the design of the patch (with $f_r =$ resonant frequency of the patch, $c =$ velocity of light in free space, $L =$ average length of the patch, and $H =$ height of the patch). The analytical length of a 8.5 mm height quarter-wavelength resonator is then found to be 71.7 mm at 935 MHz in the GSM band. This length can be slightly reduced by using a partial shorting strip instead of a plain shorting wall. Moreover, it has been previously shown that both the antenna with its feeding and shorting pins always have to be positioned at the top of the PCB to obtain an efficient antenna-chassis combination, especially maximum bandwidth behavior [8] [9]– [11]. In such a configuration, the matching of the antenna to a 50 Ω source is not so difficult to achieve since the 50 Ω input impedance point is not spatially far from the shorting strip. However, due to its intrinsic properties, the design at 935 MHz of a rectangular quarter-wavelength patch with its length aligned with the PCB length, will only lead to an odd number of higher resonance frequencies namely 2805 MHz (3 f_r), 4675 MHz (5 f_r), and so on. As our main element need to resonate in the 1710–2170 MHz band, we need to decrease the working frequency of the 3rd higher mode of this structure. It has been successfully demonstrated in [9] that adding a capacitive load to the structure will result in a decrease of the frequency of its higher modes. This can be achieved by folding the patch over on itself. The value of this capacitance can be controlled by increasing or decreasing the metal facing surfaces. However, this folding operation also reduces the bandwidth of the antenna due to an inherent increase of its total quality factor Q [12].

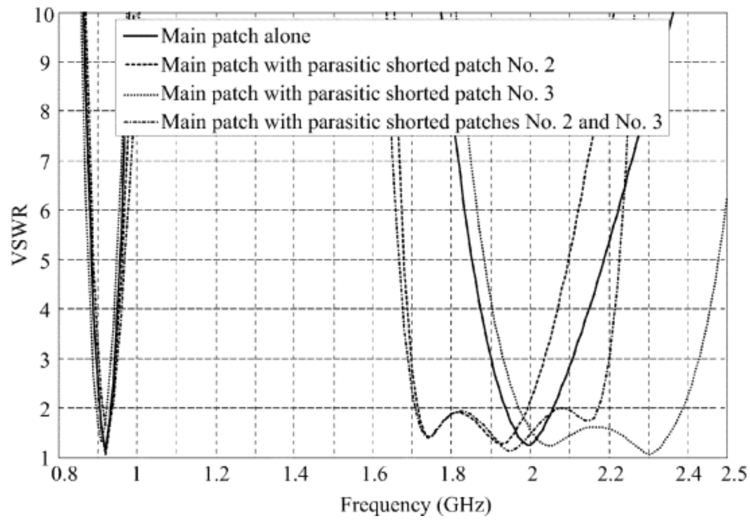

Fig. 2. Simulated VSWR of the main patch with and without parasitic shorted patches no. 2 and no. 3.

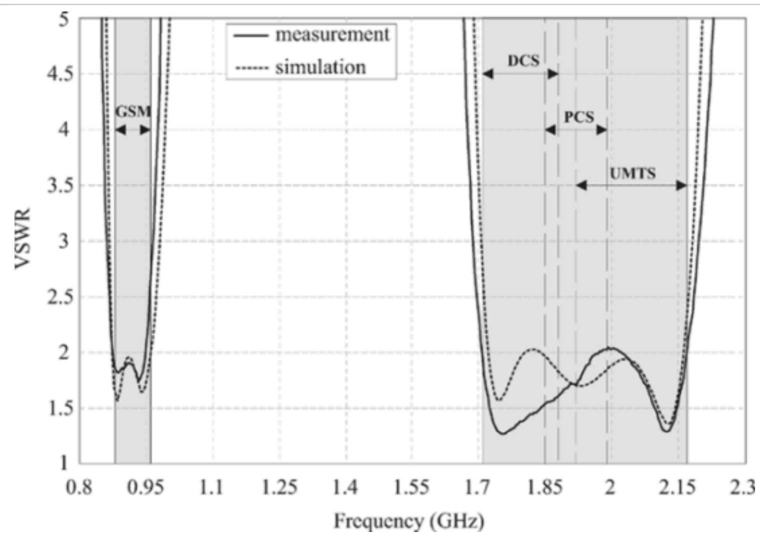

Fig. 3. Measured and simulated VSWR of the quad-band antenna.

Three parasitic elements have to be added to the main patch to achieve our desired multiband goal. These elements are chosen quarter-wavelength type, each connected to the ground plane by metallic strips and located near the main patch in order to be correctly electromagnetically excited. Capacitive loads can be added to these parasitic patches by vertically folding their strip ends. Hence, the electrical lengths of these resonators are artificially increased without enlarging the whole antenna size. A first parasitic patch have to be added to enlarge the GSM bandwidth (no. 1 on Fig. 1), its theoretical quarter-wavelength is found to be 76 mm at 888 MHz. Two others parasitic patches must be added to increase the upper bandwidth (no. 2 and no. 3 on Fig. 1). Their theoretical lengths are 34.1 mm at 1760 MHz and 26.9 mm at 2120 MHz.

SECTION III.
Results

With these empirical design rules, a dual-band patch antenna was first designed and optimized using a simulation tool based on the method of moments : IE3D [13]. Parasitic patches no. 2 and no. 3 were then separately and simultaneously added to this main patch. At last, parasitic patch no. 1 was built to achieve the final goal. All structures have been fine tuned to achieve the best possible coupling between the resonances i.e the largest possible bandwidths. This tuning was made by slightly changing the main dimensions of the parasitic patches and/or their gaps with the main patch. All the optimized dimensions of each stage are not listed here for brevity. Fig. 2 shows the simulated VSWR of the main patch with and without parasitic shorted patches no. 2 and no. 3. It is seen on this graph that the main patch alone has two resonances in the GSM band and around 2 GHz with both small bandwidths. The VSWR curves of the main patch with the addition of only one parasitic patch (no. 2 or no. 3) are also plotted on this graph. In both cases, it increases the upper bandwidth of the first antenna in two different ways: parasitic no. 2 works below the 3rd resonance of the main patch while parasitic No. 3 works above. The simulated VSWR of the main plate with the simultaneous addition of these two shorted patches is also plotted on Fig. 2. This structure has now an upper bandwidth of 470 MHz (1705–2175 MHz) with a VSWR less than 2 covering the DCS, PCS and UMTS standards but the lower bandwidth of 40 MHz (905–945 MHz) with a VSWR less than 2.5 is clearly insufficient to cover the entire GSM band. The performances of the main antenna with parasitics no. 2 and no. 3 shows that an additional parasitic element no. 1 is needed to increase the low part of the GSM band. Fig. 3 compares the simulated and measured VSWR of the final quad-band antenna (dimensions 38.5 mm×28.5 mm×8.5 mm).

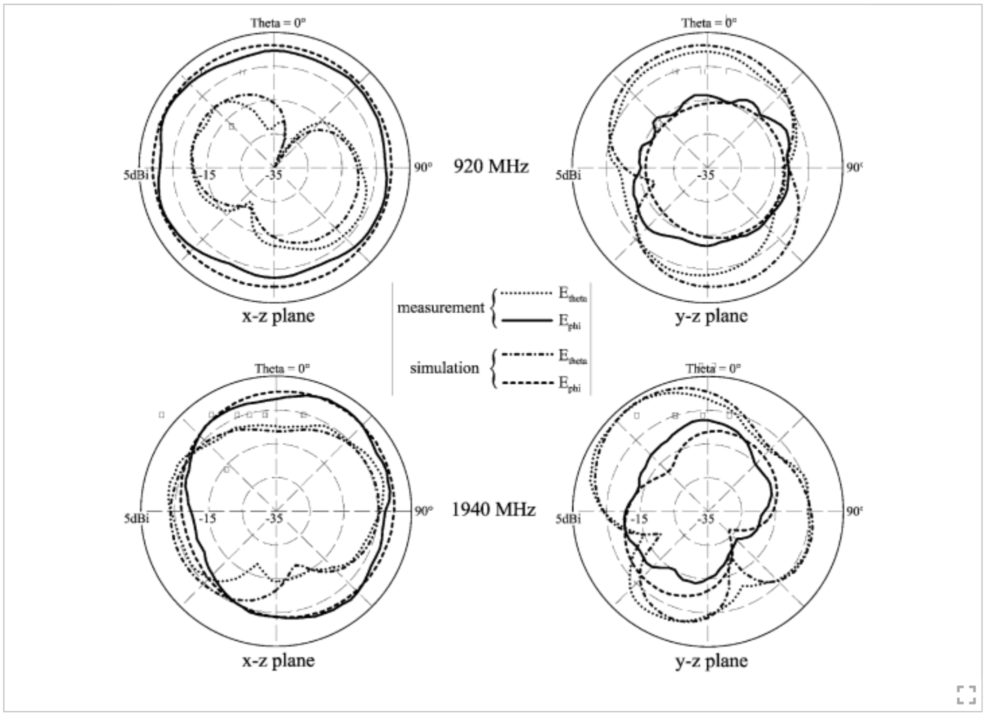

Fig. 4. Measured and simulated radiation gain patterns at 920 MHz and 1940 MHz for the quad-band antenna. Antenna orientation is given in Fig. 1.

The step by step optimization of the structure resulted in a folded dual-band patch antenna of dimensions 32 mm×22 mm×8.5 mm with a strong quasilocalized capacitive load at its end and an average quarter-wavelength length of 72.2 mm that is very close to the theoretical value of 71.7 mm. The physical length of parasitic patch no. 1 is 77.6 mm, compared with the theoretical quarter-wavelength of 76 mm at 888 MHz. Capacitive loads were added to the parasitic patches no. 1 and no. 2 by vertically folding their strip ends. Physical lengths of elements no. 2 and no. 3 are respectively 31.2 mm and 19 mm to be compared with the theoretical quarter-wavelengths of 34.1 mm at 1760 MHz and 26.9 mm at 2120 MHz. The small discrepancies between these values comes from the theoretical formula which doesn't take into account localized and distributed capacitive loading effects. This capacitive effect is very strong in the case of parasitic element no. 3 where two high impedance portions of metal face each others. A good agreement between theoretical and experimental results is observed. The measured lower bandwidth is 90 MHz (870–960 MHz) with a VSWR better than 2.5 while the upper bandwidth is 460 MHz (1710–2170 MHz) with a VSWR less than 2.

The measured and simulated radiation gain patterns of the antenna at 920 MHz and 1940 MHz are depicted in Fig. 4. These patterns reveal a quasi omnidirectional character in the x-z plane as well as a lack of polarization purity due to the radiation from the PCB. However, these two properties are not a drawback in mobile phone applications where omnidirectional radiation patterns as well as both vertical and horizontal electromagnetic field polarization occur in urban environments [14]. These omnidirectional patterns are due to the dipole-like behavior of the structure coming from the antenna-chassis combination : due to the in-phase currents flowing on the PCB in the GSM band, quasi perfect omnidirectional pattern is seen while some directivity appears at 1940 MHz in both planes since the length of the PCB is now larger than half the wavelength. Some discrepancies are found between theoretical and experimental far-field patterns. The small ripple seen in the measured curves comes principally from our measurement setup, especially from the radiation contribution of the feed cable of the antenna : in small antenna measurements, it is difficult to correctly choke the feed cable to avoid currents flowing on it [15], [16]. The measured maximum gains for the antenna are 1 dBi at 920 MHz and 3.3 dBi at 1940 MHz while the simulated are respectively 1.3 dBi and 3.5 dBi. The small discrepancies between these values are mainly attributed to the dielectric losses of the plastic support used in our radiation pattern measurement setup to maintain the antenna.

The efficiency of the structure, defined as the total radiated power divided by the incident power at the feed, takes into account reflection losses due to the mismatch between the coaxial probe and the antenna as well as ohmic losses. The computed efficiency was respectively above 69% and 74% in the GSM and DCS/PCS/UMTS bands which is suitable for mobile phone communication terminals.

SECTION IV.
Conclusion

A compact multiband PIFA antenna with parasitic elements was designed and placed on a realistic PCB ground plane. This new structure uses various techniques of miniaturization to achieve low return loss in both GSM and DCS/PCS/UMTS bands. The quasi omnidirectional gain radiation pattern characteristics with good efficiency over the covered frequency bands make this antenna suitable for mobile phone applications. Further work will be concentrated on the coverage of new 2.4 GHz and 5.2 GHz standards.

ACKNOWLEDGMENT

The authors would like to thank Prof. V. F. Fusco from the Queen's University of Belfast, Patrice Brachat from France Telecom R&D, and J. Baro for their fruitful remarks about this work.

EXHIBIT B

An Inverted FL Antenna for Dual-Frequency Operation

Hisamatsu Nakano, *Fellow, IEEE*, Yusuke Sato, Hiroaki Mimaki, *Member, IEEE*, and Junji Yamauchi, *Member, IEEE*

***Abstract*—An inverted FL antenna (InvFLA) is analyzed to obtain dual-frequency operation at 2.45 and 5.2 GHz (wireless LAN system frequencies). The InvFLA is composed of inverted FL elements, a parasitic element, and a ground plate, where these lie in the same plane, i.e., the structure is a card-type structure having a co-planar ground plate. The antenna height above the ground plate is very small: $5.5\ \mathrm{mm} = 0.045$ wavelength at 2.45 GHz. The analysis shows that the InvFLA has a 4.1% bandwidth around 2.45 GHz and a 31.8% bandwidth around 5.2 GHz, both for a $\mathrm{VSWR} = 2$ criterion. The gain is calculated to be 0.9 dBi at 2.45 GHz and 1.7 dBi at 5.2 GHz, with a small gain variation in each of the VSWR bands.**

***Index Terms*—Card-type antenna, dual-frequency operation, finite-difference time-domain (FDTD) analysis, inverted F, inverted L.**

I. INTRODUCTION

THE increasing demand for wireless communications has been accelerating development of new antennas that operate in the required frequency bands [1]–[5]. The dual-frequency antenna is one of these new antennas, and so far numerous efforts have been made in this area [6]–[8]. For example, Wong has investigated microstrip patches for dual-frequency operation and summarized them in [9].

This paper presents an antenna that responds to the above-mentioned trend: an inverted FL antenna (InvFLA) for dual-frequency operation. The InvFLA is made of a thin conducting film, having a flat structure, as shown in Fig. 1(b), where both the radiation element (inverted F and L strip lines) in the positive y space and the ground plate (GP) in the negative y space lie in the same plane (x-y plane). In other words, the InvFLA has a co-planar ground plate, forming a card-type antenna structure.

The card-type InvFLA structure differs from the layered microstrip antenna structure for dual-frequency operation in [9], where the ground plate backs a radiation element (patch element), i.e., the patch is parallel to the ground plate. It is emphasized that the card-type structure facilitates the use of the InvFLA in PC card devices for personal computers or inside mobile phone handsets.

After a brief summary of the analysis methods, which are based on the finite-difference time-domain method (FDTDM) [10], this paper investigates an InvFLA for realizing dual-frequency operation at 2.45 and 5.2 GHz (frequencies used for wireless LAN communications). Note that the final structural parameters for the InvFLA are obtained through a step-by-step investigation of the following structures: 1) an inverted L element; 2) an inverted F element; 3) a compound of the inverted L and F elements, referred to as a *compounded LF*; 4) the compounded LF with a parasitic inverted L element; and 5) the compounded LF with a *modified* parasitic inverted L element. Also, note that the design process presented in this paper is not necessarily restricted to the specific frequencies 2.45 and 5.2 GHz. It is possible to apply the same design technique to other dual-frequency antenna designs.

For confirmation of the FDTDM results (obtained using the FDTDM computer programs developed by the authors), experimental results are presented. A good agreement between the FDTDM results and the experimental results is found.

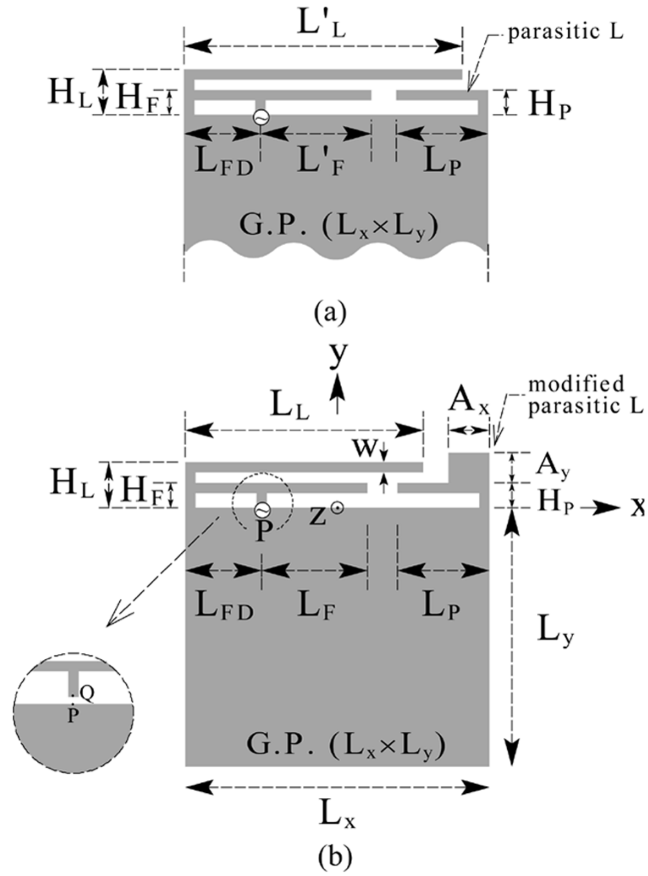

Fig. 1. Antenna structures. (a) A compound of inverted L and F elements (referred to as a *compounded LF*) with a parasitic L element above a co-planar ground plate (GP). (b) A compounded LF with a modified parasitic L element above a co-planar ground plate, referred to as the inverted FL antenna (InvFLA). The ground plate size in (a) is the same as that in (b): $L_x \times L_y = 30\ \mathrm{mm} \times 25.5\ \mathrm{mm}$.

Manuscript received December 14, 2004; revised May 22, 2005.
The authors are with the College of Engineering, Hosei University, Tokyo 184-8584, Japan (e-mail: nakano@k.hosei.ac.jp).
Digital Object Identifier 10.1109/TAP.2005.852502

II. Configuration

Fig. 1(a) shows a step involved in reaching the antenna structure of Fig. 1(b). The radiation element in Fig. 1(a) is a compound of three sub-elements: an inverted L element (see inset (I) of Fig. 2, where elements α-β-γ and α'-β'-γ' are collectively referred to as the "inverted L element"), an inverted F element (see inset (II) of Fig. 2), and a parasitic inverted L element (simply referred to as a *parasitic* L *element*).

Fig. 1(b) is a modified version of the structure in Fig. 1(a), where a small protrusion of area $A_x \times A_y$ is added to the parasitic L element in Fig. 1(a). The structure of Fig. 1(b) is based on the inverted L and F elements, and hence it is referred to as the *inverted FL antenna* (InvFLA). It is emphasized that the InvFLA is made of a thin conducting film, where the ground plate (GP) is a co-planar ground plate, i.e., the ground plate and the radiation element lie in the same plane (x-y plane), forming a card-type structure.

The heights of the radiation sub-elements (H_L, H_F, and H_P) and the ground plate size ($L_x \times L_y$) in Fig. 1(b) are the same as those in Fig. 1(a). However, the horizontal lengths L_L and L_F in Fig. 1(b) are slightly different from L'_L and L'_F in Fig. 1(a), respectively, as will be revealed later.

The InvFLA is excited at terminals P and Q, where the distance between P and Q is fixed to be 0.5 mm. The distance from the left side edge of the ground plate to terminal P is denoted as $L_{\rm FD}$. For the experimental work, the InvFLA is excited through a 50-ohm coaxial line without a balun circuit, where the inner conductor of the coaxial line is connected to point Q and the outer conductor is soldered to the ground plate. To facilitate a PC card implementation, a thin coaxial line can be used (a coaxial line whose outer diameter is 0.8 mm is commercially available).

The ground plate size and the strip line width of the radiation element are fixed to be $L_x \times L_y = 30 \text{ mm} \times 25.5 \text{ mm}$ and $w = 1 \text{ mm}$, respectively, throughout this paper. There are nine structural parameters to be determined: the heights (H_L, H_F, H_P), the strip line lengths (L_L, L_F, L_P), the protrusion size (A_x, A_y), and the feed point location $L_{\rm FD}$. In this paper, the heights (H_L, H_F, H_P) are pre-selected to be small with respect to the wavelengths at 2.45 and 5.2 GHz: $(H_L, H_F, H_P) = (4.5 \text{ mm}, 2.5 \text{ mm}, 2.5 \text{ mm})$. The remaining structural parameters (L_L, L_F, L_P), (A_x, A_y) and $L_{\rm FD}$ are to be determined for operation at 2.45 and 5.2 GHz.

III. Analysis and Discussion

Analysis is performed using the finite-difference time-domain method (FDTDM). For this, Yee's algorithm based on rectangular cells [10] is adopted, where the analysis space is terminated using Liao's second order absorbing boundary condition [11]. The antenna excitation is modeled by a delta-gap voltage source $V_{\rm in}(t)$, which is defined by a sine function modulated by a Gaussian function: $V_{\rm in}(t) = V_{\rm gauss}(t)\sin\omega t$, where $V_{\rm gauss}(t) = \exp\{-(t-T)/KT\}^2$, with $K = 0.29$ and $T = 0.646/f_{\rm 3dB}$. Note that $f_{\rm 3dB}$ is the frequency at which the power spectrum $(|\text{Fourier transform of } V_{\rm gauss}(t)|^2)$ drops 3 dB from its maximum value. The electric field at a far-field point, $E_{\rm Far}$ (composed of E_θ and E_ϕ), is calculated on the basis of the equivalence principle [12].

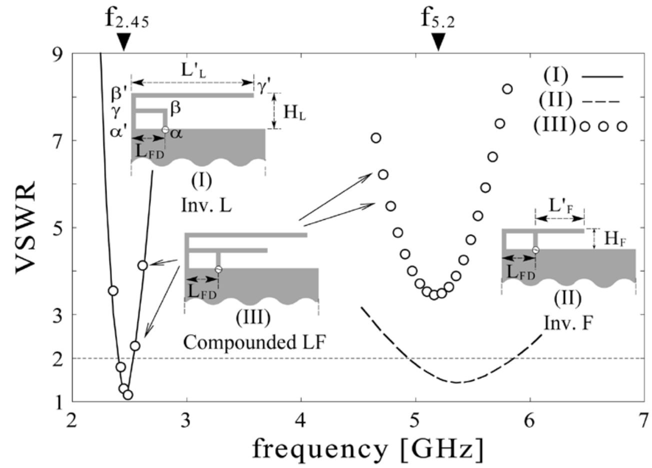

Fig. 2. VSWRs of three structures. The structural parameters for an inverted L element (I) are $(H_L,\ L'_L) = (4.5 \text{ mm},\ 27.5 \text{ mm})$ and $L_{\rm FD} = 7.5 \text{ mm}$, and those for an inverted F element (II) are $(H_F,\ L'_F) = (2.5 \text{ mm},\ 11 \text{ mm})$ and $L_{\rm FD} = 7.5 \text{ mm}$. A compounded LF (III) has the same structural parameters used for the sub- elements (I) and (II). The ground plate sizes in structures (I), (II), and (III) are the same: $L_x \times L_y = 30\text{mm} \times 25.5 \text{ mm}$.

The InvFLA is intended for installation in *mobile* equipment. In such a case, polarization purity (low cross polarization) is not required; however, an appropriate VSWR frequency response must be realized. The structural parameters for the InvFLA, Fig. 1(b), are obtained through the five steps described below, where the first three steps are rough adjustments and the fourth and fifth steps are devoted to a fine-tuning of the design.

For the first step, the inverted L element [see inset (I) of Fig. 2] is analyzed for a height of $H_L = 4.5\text{mm} = 0.0368\lambda_{2.45}$, pre-selected in Section II, where $\lambda_{2.45}$ is the wavelength at 2.45 GHz ($\equiv f_{2.45}$). To obtain resonance around $f_{2.45}$, the horizontal length L'_L is chosen such that the total length $H_L + L'_L$ is close to one-quarter wavelength at $f_{2.45}$: $L'_L = 27.5 \text{ mm}$ $(H_L + L'_L = 32 \text{ mm} = 0.261\lambda_{2.45})$. Resonance at $f_{2.45}$ is realized by adjusting the location of feed point (distance $L_{\rm FD}$). The VSWR frequency response for $L_{\rm FD} = 7.5 \text{ mm}$ is shown by the solid line in Fig. 2.

The second step is performed using the inverted F element shown in inset (II) of Fig. 2. The height H_F is chosen to be smaller than H_L for the inverted L element, described in Section II: $H_F = 2.5 \text{ mm} = 0.0433\lambda_{5.2}$, where $\lambda_{5.2}$ is the wavelength at 5.2 GHz ($\equiv f_{5.2}$). The feed point is located at the same point as that for the aforementioned inverted L element ($L_{\rm FD} = 7.5 \text{ mm}$). Resonance around $f_{5.2}$ is obtained by choosing the horizontal length L'_F such that the $H_F + L'_F$ is close to one-quarter wavelength at $f_{5.2}$: $L'_F = 11 \text{ mm}$ $(H_F + L'_F = 13.5 \text{ mm} = 0.234\lambda_{5.2})$. The VSWR for this structure is shown by the broken line in Fig. 2. Note that the horizontal lengths L'_F (obtained in the second step) and L'_L (obtained in the first step) are slightly changed to L_F and L_L, respectively, after the fine-tuning in the fifth step.

The third step is to compound the inverted L and F elements determined in the first and second steps, as shown in inset (III) of Fig. 2. The white dots in Fig. 2 show the VSWR for this structure. It is observed that the VSWR at $f_{2.45}$ remains almost unchanged; however the VSWR at $f_{5.2}$ deteriorates due to mutual

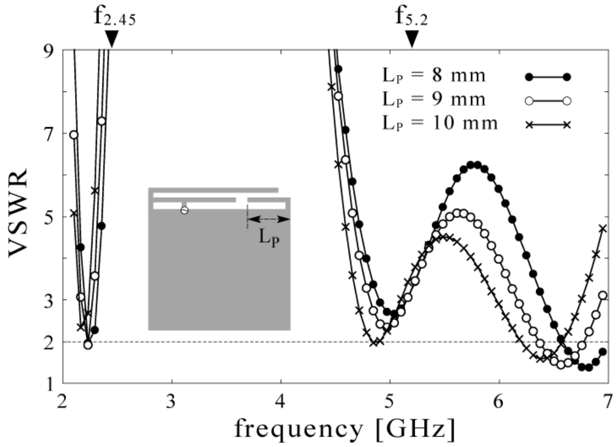

Fig. 3. Effects of the length of a parasitic L element, L_P, on the VSWR, where the structural parameters $(H_L, L'_L) = (4.5\ \text{mm},\ 27.5\ \text{mm})$, $(H_F, L'_F) = (2.5\ \text{mm},\ 11\ \text{mm})$, and $L_{\text{FD}} = 7.5\ \text{mm}$ are used. The ground plate size is $L_x \times L_y = 30\ \text{mm} \times 25.5\ \text{mm}$.

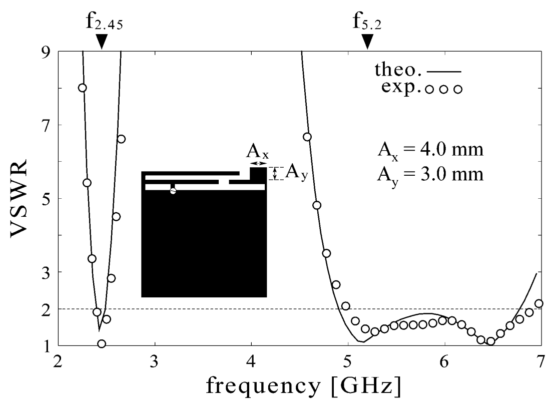

Fig. 4. VSWR for an inverted FL antenna. The structural parameters are $(H_L, L_L) = (4.5\ \text{mm},\ 24.5\ \text{mm})$, $(H_F, L_F) = (2.5\ \text{mm},\ 10.5\ \text{mm})$, $L_{\text{FD}} = 7.5\ \text{mm}$, $(H_P, L_P) = (2.5\ \text{mm},\ 9.0\ \text{mm})$, $(A_x, A_y) = (4.0\ \text{mm},\ 3.0\ \text{mm})$, and $(L_x \times L_y) = (30\ \text{mm} \times 25.5\ \text{mm})$.

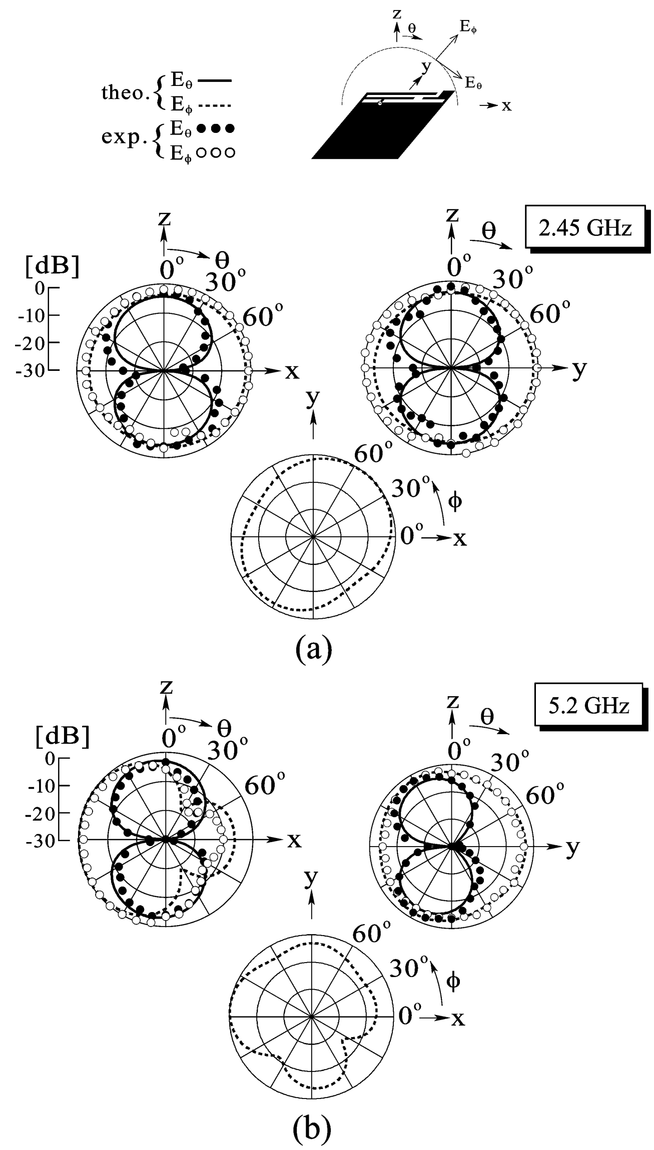

Fig. 5. Radiation patterns of an inverted FL antenna. (a) At 2.45 GHz. (b) At 5.2 GHz. The structural parameters are $(H_L, L_L) = (4.5\ \text{mm},\ 24.5\ \text{mm})$, $(H_F, L_F) = (2.5\ \text{mm},\ 10.5\ \text{mm})$, $L_{\text{FD}} = 7.5\ \text{mm}$, $(H_P, L_P) = (2.5\ \text{mm},\ 9.0\ \text{mm})$, $(A_x, A_y) = (4.0\ \text{mm},\ 3.0\ \text{mm})$, and $(L_x \times L_y) = (30\ \text{mm} \times 25.5\ \text{mm})$.

effects between the inverted L and F elements. This is overcome in the following fourth and fifth steps.

In the fourth step, a parasitic L element is added to the structure discussed in the third step, as shown in Fig. 1(a). The height of the parasitic L element is chosen to be equal to that of the inverted F element, as described in Section II: $H_P = H_F = 2.5\ \text{mm}$. Fig. 3 shows the VSWR as a function of frequency for three values of the horizontal length of the parasitic L element, L_P, where the structural parameters for the inverted L and F elements are held at the values used in the third step: $(H_L, L'_L) = (4.5\ \text{mm},\ 27.5\ \text{mm})$, $(H_F, L'_F) = (2.5\ \text{mm},\ 11\ \text{mm})$, and $L_{\text{FD}} = 7.5\ \text{mm}$. It is found that the parasitic L element generates resonances between 6 and 7 GHz. Note that the total length of the parasitic L, $H_P + L_P$, is close to one-quarter wavelength at the frequency where the minimum VSWR for each L_P appears: $H_P + L_P = 0.238\lambda_{6.8}$ at 6.8 GHz for $L_P = 8\ \text{mm}$, $H_P + L_P = 0.253\lambda_{6.6}$ at 6.6 GHz for $L_P = 9\ \text{mm}$, and $H_P + L_P = 0.267\lambda_{6.4}$ at 6.4 GHz for $L_P = 10\ \text{mm}$, where λ_f is the wavelength at frequency f.

At this point there are two issues: 1) the VSWR curve is slightly shifted downward with respect to frequencies $f_{2.45}$ and $f_{5.2}$; and 2) the VSWR around $f_{5.2}$ is still larger than 2. These issues are solved by the following structural modifications: 1) reduction of the original horizontal strip line lengths L'_L and L'_F, and 2) widening of the strip width of the parasitic L element. Note that the widening of the strip width is realized by making a protrusion on the parasitic L element, where part of the strip line is widened to $w + A_y$ over length A_x, as shown in Fig. 1(b).

The fifth step is to perform the aforementioned structural modifications for dual-frequency operation at 2.45 and 5.2 GHz. Using trial and error, the structural parameters are determined to be $(L_L, L_F, L_P) = (24.5\ \text{mm},\ 10.5\ \text{mm}, 9.0\ \text{mm})$,

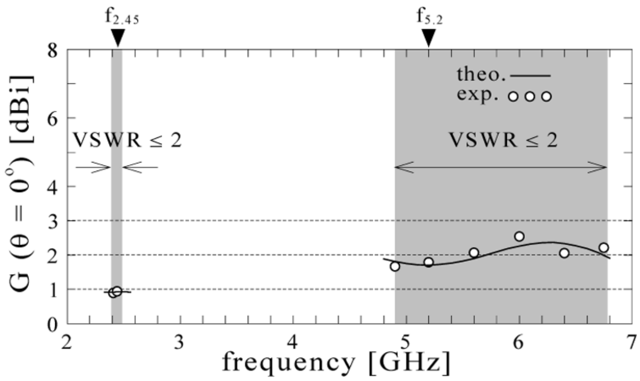

Fig. 6. Gain in the z-direction of an inverted FL antenna. The structural parameters are $(H_L, L_L) = (4.5\ \mathrm{mm},\ 24.5\ \mathrm{mm})$, $(H_F, L_F) = (2.5\ \mathrm{mm},\ 10.5\ \mathrm{mm})$, $L_{\mathrm{FD}} = 7.5\ \mathrm{mm}$, $(H_P, L_P) = (2.5\ \mathrm{mm},\ 9.0\ \mathrm{mm})$, $(A_x, A_y) = (4.0\ \mathrm{mm},\ 3.0\ \mathrm{mm})$, and $(L_x \times L_y) = (30\ \mathrm{mm} \times 25.5\ \mathrm{mm})$.

$(A_x, A_y) = (4.0\ \mathrm{mm},\ 3.0\ \mathrm{mm})$, and $L_{\mathrm{FD}} = 7.5\ \mathrm{mm}$. Note that the horizontal lengths L_L and L_F are slightly smaller than the original lengths L'_L and L'_F in Fig. 1(a), respectively. Also note that the largest antenna height $(H_P + A_y)$ is very small with respect to the wavelength: $5.5\ \mathrm{mm} = 0.045$ wavelength at 2.45 GHz. Fig. 4 shows the frequency response of the VSWR for the InvFLA defined with these final values for the structural parameters. This figure clearly indicates dual-frequency operation at $f_{2.45}$ and $f_{5.2}$. The frequency bandwidth for a $\mathrm{VSWR} = 2$ criterion is 4.1% for the $f_{2.45}$ band and 31.8% for the $f_{5.2}$ band. The results are confirmed by the experimental results (white dots).

Fig. 5 shows the radiation patterns at $f_{2.45}$ and $f_{5.2}$. For confirmation of the FDTDM results, experimental results in the principal planes (x-z and y-z planes) are presented. Additionally, only the FDTDM results of the radiation patterns in the x-y plane at $f_{2.45}$ and $f_{5.2}$ are presented for completeness. The radiation patterns are useful in understanding the gain characteristic in the z direction $G(\theta = 0°)$, which is shown in Fig. 6 together with experimental results, where the shadowed areas in the figure show the VSWR bands. It is found that the gain (with respect to an isotropic source) is approximately 0.9 dBi at $f_{2.45}$ and approximately 1.7 dBi at $f_{5.2}$, with a small gain variation in each VSWR band. These gain values are small due to the fact that the radiation is not highly directive, as seen from the radiation pattern E_ϕ.

The difference between the gains at $f_{2.45}$ and $f_{5.2}$ (i.e., the gain in the z-direction at 2.45 GHz is smaller than that at 5.2 GHz) is attributed to the following facts: 1) the radiation pattern E_ϕ at 2.45 GHz in each of the x-z and y-z planes is more omnidirectional than that at 5.2 GHz and 2) the radiation pattern E_θ at 2.45 GHz in each of the x-z and y-z planes (having a figure-eight pattern) shows a wider half-power beam width than that at 5.2 GHz.

An omnidirectional pattern is desirable for communications between a fixed base station antenna and an antenna installed in a *mobile* device. Note that, if a more omnidirectional E_ϕ pattern (in the x-z plane) is required for the InvFLA at 5.2 GHz, this can be achieved by placing the parasitic L element just under the horizontal strip line of the inverted F [13].

IV. Conclusion

An InvFLA, made of a thin conducting film, has a card-type structure, where the radiation element is a compound of inverted L and F elements, which is adjacent to a co-planar ground plate. The design procedure for dual-frequency operation at $f = 2.45$ GHz and 5.2 GHz is described in five steps. In the first step, an inverted L element is designed for operation at 2.45 GHz. In the second step, an inverted F is designed for operation at 5.2 GHz. Based on these designs, a compound of the inverted L and F elements is investigated in the third step. Fine adjustment for dual-frequency operation is performed by introducing a parasitic L element in the fourth step and then modifying the parasitic L element in the fifth step.

It is found that the VSWR frequency bandwidth of the InvFLA is 4.1% around 2.45 GHz and 31.8% around 5.2 GHz. It is also revealed that the E_ϕ component of the radiation field from the InvFLA spreads out in a somewhat omnidirectional fashion. Further analysis shows that the gain variation in each VSWR band is small. The gain in the z direction (normal to the antenna plane) is 0.9 dBi at 2.45 GHz and 1.7 dBi at 5.2 GHz.

Acknowledgment

The authors would like to thank V. Shkawrytko for his invaluable help in the preparation of this manuscript.

References

[1] Y. Guo, M. Y. W. Chia, and Z. N. Chen, "Miniature built-in quad-band antennas for mobile handsets," *IEEE Antennas Wireless Propag. Lett.*, vol. 2, pp. 30–32, 2003.

[2] M. Ali, G. J. Hayes, H. Hwang, and R. A. Sadler, "Design of multiband internal antenna for third generation mobile phone handsets," *IEEE Trans. Antennas Propag.*, vol. 51, no. 7, pp. 1452–1461, Jul. 2003.

[3] Y. Guo, I. Ang, and M. Y. W. Chia, "Compact internal multiband antennas for mobile handsets," *IEEE Antennas Wireless Propag. Lett.*, vol. 2, pp. 143–146, 2003.

[4] M. F. Abedin and M. Ali, "Modifying the ground plane and its effect on planar inverted-F antennas (PIFA's) for mobile phone handsets," *IEEE Antennas Wireless Propag. Lett.*, vol. 2, pp. 226–229, 2003.

[5] Y. Kwon, J. Moon, and S. Park, "An internal triple-band planar inverted-F antenna," *IEEE Antennas Wireless Propag. Lett.*, vol. 2, pp. 341–344, 2003.

[6] D. Llorens, P. Otero, and C. C-Penalosa, "Dual-band, single CPW port, planar-slot antenna," *IEEE Trans. Antennas Propag.*, vol. 51, no. 1, pp. 137–139, Jan. 2003.

[7] S. Yeh, K. Wong, T. Chiou, and S. Fang, "Dual-band planar inverted F antenna for GSM/DCS mobile phones," *IEEE Trans. Antennas Propag.*, vol. 51, no. 5, pp. 1124–1126, May 2003.

[8] H. Chen, W. Chen, Y. Cheng, and Y. Lin, "Dualband meander monopole antenna," in *Proc. IEEE Antennas and Propagation Soc. Int. Symp.*, vol. 3, Columbus, OH, Jun. 2003, pp. 48–51.

[9] K. Wong, *Compact and Broadband Microstrip Antennas*. New York: Wiley, 2002.

[10] A. Taflove, *Computational Electrodynamics: The Finite-Difference Time Domain Method*. Norwood, MA: Artech House, 1995.

[11] Z. P. Liao, H. L. Wong, B. P. Yang, and Y. F. Yuan, "A transmitting boundary for transient wave analysis," *Science Sinica, Series A*, vol. 27, no. 10, pp. 1063–1076, 1984.

[12] C. A. Balanis, *Antenna Theory: Analysis and Design*, 2nd ed: Wiley, 1982, pp. 575–594.

[13] H. Nakano, K. Morishita, Y. Sato, H. Mimaki, and J. Yamauchi. A card-type inverted LFL antenna for dual-frequency operation. presented at Proc. IEEE-ACES Int. Conf. Wireless Communications and Applied Computational Electromagnetics. [CD-ROM] s27p03i

Hisamatsu Nakano (M'75–SM'87–F'92) was born in Ibaraki, Japan, on April 13, 1945. He received the B.E., M.E., and Dr.E. degrees in electrical engineering from Hosei University, Tokyo, Japan, in 1968, 1970, and 1974, respectively.

Since 1973, he has been a Member of the Faculty of Hosei University, where he is now a Professor of Electronic Informatics. He was a Visiting Associate Professor from March to September 1981, at Syracuse University, Syracuse, NY. He was a Visiting Professor from March to September 1986, at the University of Manitoba, Canada, and from September 1986 to March 1987, at the University of California, Los Angeles. In 2001, he was appointed to the Guest Professorship of Shanghai Jiao Tong University, China. His research topics include numerical methods for low- and high-frequency antennas and optical waveguides. He has published more than 200 refereed journal papers, more than 180 international symposium papers, and more than 550 national symposium papers. He is the author of *Helical and Spiral Antennas* (New York: Research Studies Press, Wiley, 1987) and *Helical and Spiral Antennas* in *Encyclopedia of Telecommunications* (New York: Wiley, 2002) and is the coauthor of *Analysis Methods of Electromagnetic Wave Problems, Volume Two* (Norwood, MA: Artech House, 1996).

Prof. Nakano received the Institution of Electrical Engineers (IEE) International Conference on Antennas and Propagation Best Paper Award and the IEEE TRANSACTIONS ON ANTENNAS AND PROPAGATION Best Application Paper Award (H. A. Wheeler Award) in 1989 and 1994, respectively. In 1992, he was elected an IEEE fellow for contributions to the design of spiral and helical antennas. In 2001, he received the Award of Distinguished Technical Communication, from the Society for Technical Communication, USA. He is an Associate Editor of several journals and magazines, such as *Electromagnetics*, *IEEE Antennas and Propagation Magazine*, *IEEE Antennas and Wireless Propagation Letters*, and *Asian Information-Science-Life*.

Yusuke Sato was born in Saitama, Japan, on August 14, 1981. He received the B.E. degree in electrical engineering from Hosei University, Tokyo, Japan, in 2004, where he is currently working toward the M.E. degree.

Mr. Sato is a Member of the Institute of Electronics, Information and Communication Engineers (IEICE) of Japan.

Hiroaki Mimaki (M'83) received the B.E. degree in electrical engineering from Tokyo Denki University, Tokyo, Japan, in 1976 and the M.E. degree in electrical engineering from Hosei University, Tokyo, Japan, in 1981.

He is currently an Assistant at Hosei University. His research interests are in thin wire antennas.

Mr. Mimaki is a Member of the Institute of Electronics, Information and Communication Engineers (IEICE) of Japan.

Junji Yamauchi (M'85) was born in Nagoya, Japan, on August 23, 1953. He received the B.E., M.E., and Dr.E. degrees from Hosei University, Tokyo, Japan, in 1976, 1978, and 1982, respectively.

From 1984 to 1988, he served as a Lecturer in the Electrical Engineering Department of Tokyo Metropolitan Technical College. Since 1988, he has been a Member of the Faculty of Hosei University, where he is now a Professor of Electronic Informatics. He is the author of the book *Propagating Beam Analysis of Optical Waveguides* (Hertfordshire, U.K.: Research Studies Press, 2003). His research interests include optical waveguides and circularly polarized antennas.

Dr. Yamauchi is a Member of the Optical Society of America (OSA) and the Institute of Electronics, Information and Communication Engineers (IEICE) of Japan.

EXHIBIT B
ABSTRACT

An inverted FL antenna for dual-frequency operation

H. Nakano ; Y. Sato ; H. Mimaki ; J. Yamauchi All Authors

Abstract:
An inverted FL antenna (InvFLA) is analyzed to obtain dual-frequency operation at 2.45 and 5.2 GHz (wireless LAN system frequencies). The InvFLA is composed of inverted FL elements, a parasitic element, and a ground plate, where these lie in the same plane, i.e., the structure is a card-type structure having a co-planar ground plate. The antenna height above the ground plate is very small: 5.5 mm=0.045 wavelength at 2.45 GHz. The analysis shows that the InvFLA has a 4.1% bandwidth around 2.45 GHz and a 31.8% bandwidth around 5.2 GHz, both for a VSWR=2 criterion. The gain is calculated to be 0.9 dBi at 2.45 GHz and 1.7 dBi at 5.2 GHz, with a small gain variation in each of the VSWR bands.

Published in: IEEE Transactions on Antennas and Propagation (Volume: 53 , Issue: 8, August 2005)

Page(s): 2417 - 2421

DOI: 10.1109/TAP.2005.852502

Date of Publication: 08 August 2005

Publisher: IEEE

ISSN Information:

SECTION I.
Introduction

The increasing demand for wireless communications has been accelerating development of new antennas that operate in the required frequency bands [1]– [5]. The dual-frequency antenna is one of these new antennas, and so far numerous efforts have been made in this area [6]– [8]. For example, Wong has investigated microstrip patches for dual-frequency operation and summarized them in [9].

This paper presents an antenna that responds to the above-mentioned trend: an inverted FL antenna (InvFLA) for dual-frequency operation. The InvFLA is made of a thin conducting film, having a flat structure, as shown in Fig. 1(b), where both the radiation element (inverted F and L strip lines) in the positive y space and the ground plate (GP) in the negative y space lie in the same plane (x-y plane). In other words, the InvFLA has a co-planar ground plate, forming a card-type antenna structure.

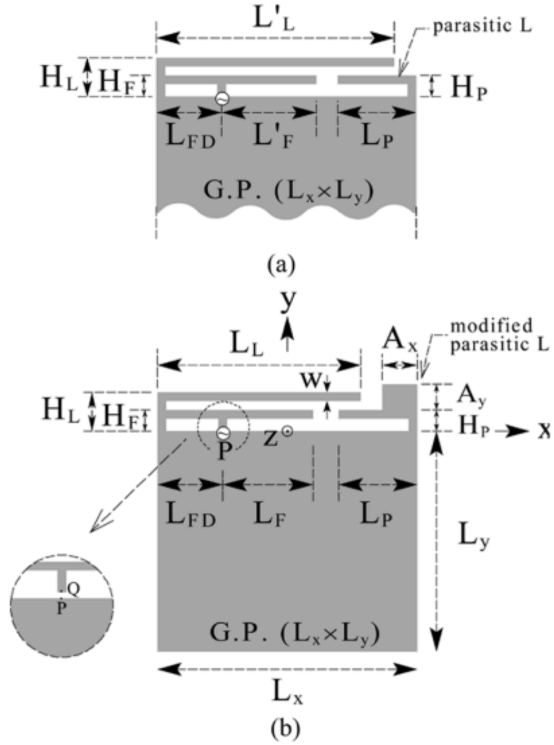

Fig. 1. Antenna structures. (a) A compound of inverted L and F elements (referred to as a *compounded LF*) with a parasitic L element above a co-planar ground plate (GP). (b) A compounded LF with a modified parasitic L element above a co-planar ground plate, referred to as the inverted FL antenna (InvFLA). The ground plate size in (a) is the same as that in (b): $L_x \times L_y = 30\ \mathrm{mm} \times 25.5\ \mathrm{mm}.$

The card-type InvFLA structure differs from the layered microstrip antenna structure for dual-frequency operation in [9], where the ground plate backs a radiation element (patch element), i.e., the patch is parallel to the ground plate. It is emphasized that the card-type structure facilitates the use of the InvFLA in PC card devices for personal computers or inside mobile phone handsets.

After a brief summary of the analysis methods, which are based on the finite-difference time-domain method (FDTDM) [10], this paper investigates an InvFLA for realizing dual-frequency operation at 2.45 and 5.2 GHz (frequencies used for wireless LAN communications). Note that the final structural parameters for the InvFLA are obtained through a step-by-step investigation of the following structures: 1) an inverted L element; 2) an inverted F element; 3) a compound of the inverted L and F elements, referred to as a *compounded LF*; 4) the compounded LF with a parasitic inverted L element; and 5) the compounded LF with a *modified* parasitic inverted L element. Also, note that the design process presented in this paper is not necessarily restricted to the specific frequencies 2.45 and 5.2 GHz. It is possible to apply the same design technique to other dual-frequency antenna designs.

For confirmation of the FDTDM results (obtained using the FDTDM computer programs developed by the authors), experimental results are presented. A good agreement between the FDTDM results and the experimental results is found.

SECTION II.
Configuration

Fig. 1(a) shows a step involved in reaching the antenna structure of Fig. 1(b). The radiation element in Fig. 1(a) is a compound of three sub-elements: an inverted L element (see inset (I) of Fig. 2, where elements

α-β-γ and α'-β'-γ' are collectively referred to as the "inverted L element"), an inverted F element (see inset (II) of Fig. 2), and a parasitic inverted L element (simply referred to as a *parasitic L element*).

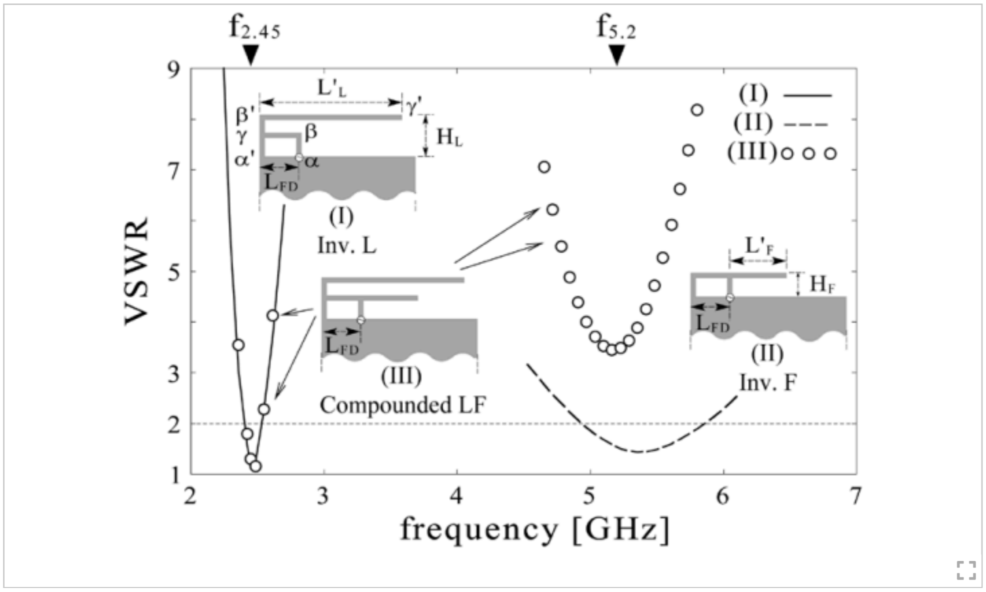

Fig. 2. VSWRs of three structures. The structural parameters for an inverted L element (I) are $(H_L,\ L'_L) = (4.5\ \text{mm},\ 27.5\ \text{mm})$ and $L_{\text{FD}} = 7.5\ \text{mm}$, and those for an inverted F element (II) are $(H_F,\ L'_F) = (2.5\ \text{mm},\ 11\ \text{mm})$ and $L_{\text{FD}} = 7.5\ \text{mm}$. A compounded LF (III) has the same structural parameters used for the sub- elements (I) and (II). The ground plate sizes in structures (I), (II), and (III) are the same: $L_x \times L_y = 30\text{mm} \times 25.5\ \text{mm}$.

Fig. 1(b) is a modified version of the structure in Fig. 1(a), where a small protrusion of area $A_x \times A_y$ is added to the parasitic L element in Fig. 1(a). The structure of Fig. 1(b) is based on the inverted L and F elements, and hence it is referred to as the *inverted FL antenna* (InvFLA). It is emphasized that the InvFLA is made of a thin conducting film, where the ground plate (GP) is a co-planar ground plate, i.e., the ground plate and the radiation element lie in the same plane (x-y plane), forming a card-type structure.

The heights of the radiation sub-elements (H_L, H_F, and H_P) and the ground plate size $(L_x \times L_y)$ in Fig. 1(b) are the same as those in Fig. 1(a). However, the horizontal lengths L_L and L_F in Fig. 1(b) are slightly different from L'_L and L'_F in Fig. 1(a), respectively, as will be revealed later.

The InvFLA is excited at terminals P and Q, where the distance between P and Q is fixed to be 0.5 mm. The distance from the left side edge of the ground plate to terminal P is denoted as L_{FD}. For the experimental work, the InvFLA is excited through a 50-ohm coaxial line without a balun circuit, where the inner conductor of the coaxial line is connected to point Q and the outer conductor is soldered to the ground plate. To facilitate a PC card implementation, a thin coaxial line can be used (a coaxial line whose outer diameter is 0.8 mm is commercially available).

The ground plate size and the strip line width of the radiation element are fixed to be $L_x \times L_y = 30\ \text{mm} \times 25.5\ \text{mm}$ and $w = 1\ \text{mm}$, respectively, throughout this paper. There are nine structural parameters to be determined: the heights (H_L, H_F, H_P), the strip line lengths (L_L, L_F, L_P), the protrusion size (A_x, A_y), and the feed point location L_{FD}. In this paper, the heights (H_L, H_F, H_P) are pre-selected to be small with respect to the wavelengths at 2.45 and 5.2 GHz: $(H_L, H_F, H_P) = (4.5\ \text{mm},\ 2.5\ \text{mm},\ 2.5\ \text{mm})$. The remaining structural parameters (L_L, L_F, L_P), (A_x, A_y) and L_{FD} are to be determined for operation at 2.45 and 5.2 GHz.

SECTION III.
Analysis and Discussion

Typesetting math: 100%

Analysis is performed using the finite-difference time-domain method (FDTDM). For this, Yee's algorithm based on rectangular cells [10] is adopted, where the analysis space is terminated using Liao's second order absorbing boundary condition [11]. The antenna excitation is modeled by a delta-gap voltage source $V_{\mathrm{in}}(t)$, which is defined by a sine function modulated by a Gaussian function: $V_{\mathrm{in}}(t) = V_{\mathrm{gauss}}(t)\sin\omega t$, where $V_{\mathrm{gauss}}(t) = \exp\{-(t-T)/KT\}^2$, with $K = 0.29$ and $T = 0.646/f_{3\mathrm{dB}}$. Note that $f_{3\mathrm{dB}}$ is the frequency at which the power spectrum ($|$Fourier transform of $V_{\mathrm{gauss}}(t)|^2$) drops 3 dB from its maximum value. The electric field at a far-field point, E_{Far} (composed of E_θ and E_ϕ), is calculated on the basis of the equivalence principle [12].

The InvFLA is intended for installation in *mobile* equipment. In such a case, polarization purity (low cross polarization) is not required; however, an appropriate VSWR frequency response must be realized. The structural parameters for the InvFLA, Fig. 1(b), are obtained through the five steps described below, where the first three steps are rough adjustments and the fourth and fifth steps are devoted to a fine-tuning of the design.

For the first step, the inverted L element [see inset (I) of Fig. 2] is analyzed for a height of $H_L = 4.5\mathrm{mm} = 0.0368\lambda_{2.45}$, pre-selected in Section II, where $\lambda_{2.45}$ is the wavelength at 2.45 GHz ($\equiv f_{2.45}$). To obtain resonance around $f_{2.45}$, the horizontal length L'_L is chosen such that the total length $H_L + L'_L$ is close to one-quarter wavelength at $f_{2.45}$: $L'_L = 27.5$ mm ($H_L + L'_L = 32$ mm $= 0.261\lambda_{2.45}$). Resonance at $f_{2.45}$ is realized by adjusting the location of feed point (distance L_{FD}). The VSWR frequency response for $L_{\mathrm{FD}} = 7.5$ mm is shown by the solid line in Fig. 2.

The second step is performed using the inverted F element shown in inset (II) of Fig. 2. The height H_F is chosen to be smaller than H_L for the inverted L element, described in Section II: $H_F = 2.5$ mm $= 0.0433\lambda_{5.2}$, where $\lambda_{5.2}$ is the wavelength at 5.2 GHz ($\equiv f_{5.2}$). The feed point is located at the same point as that for the aforementioned inverted L element ($L_{\mathrm{FD}} = 7.5$ mm). Resonance around $f_{5.2}$ is obtained by choosing the horizontal length L'_F such that the $H_F + L'_F$ is close to one-quarter wavelength at $f_{5.2}$: $L'_F = 11$ mm ($H_F + L'_F = 13.5$ mm $= 0.234\lambda_{5.2}$). The VSWR for this structure is shown by the broken line in Fig. 2. Note that the horizontal lengths L'_F (obtained in the second step) and L'_L (obtained in the first step) are slightly changed to L_F and L_L, respectively, after the fine-tuning in the fifth step.

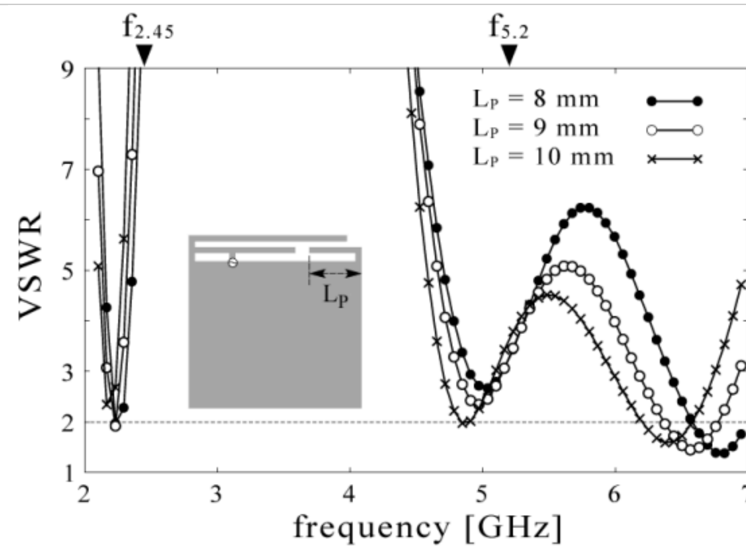

Fig. 3. Effects of the length of a parasitic L element, L_P, on the VSWR, where the structural parameters $(H_L, L'_L) = (4.5\ \mathrm{mm},\ 27.5\ \mathrm{mm})$, $(H_F, L'_F) = (2.5\ \mathrm{mm},\ 11\ \mathrm{mm})$, and $L_{\mathrm{FD}} = 7.5\ \mathrm{mm}$ are used. The ground plate size is $L_x \times L_y = 30\ \mathrm{mm} \times 25.5\ \mathrm{mm}$.

Typesetting math: 100%

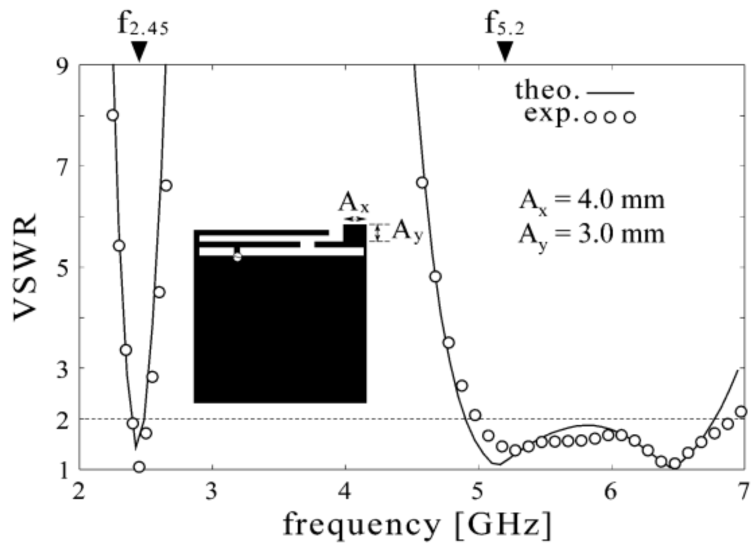

Fig. 4. VSWR for an inverted FL antenna. The structural parameters are $(H_L, L_L) = (4.5\text{ mm},\ 24.5\text{ mm})$, $(H_F, L_F) = (2.5\text{ mm},\ 10.5\text{ mm})$, $L_{\mathrm{FD}} = 7.5\text{ mm}$, $(H_P, L_P) = (2.5\text{ mm},\ 9.0\text{ mm})$, $(A_x, A_y) = (4.0\text{ mm},\ 3.0\text{ mm})$, and $(L_x \times L_y) = (30\text{ mm} \times 25.5\text{ mm})$.

The third step is to compound the inverted L and F elements determined in the first and second steps, as shown in inset (III) of Fig. 2. The white dots in Fig. 2 show the VSWR for this structure. It is observed that the VSWR at $f_{2.45}$ remains almost unchanged; however the VSWR at $f_{5.2}$ deteriorates due to mutual effects between the inverted L and F elements. This is overcome in the following fourth and fifth steps.

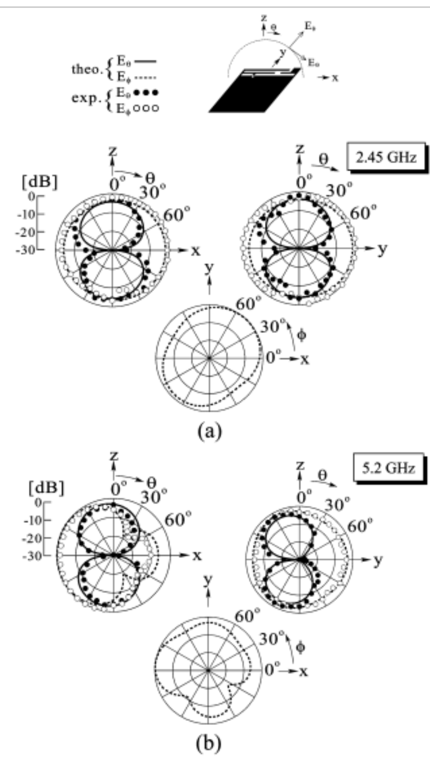

Fig. 5. Radiation patterns of an inverted FL antenna. (a) At 2.45 GHz. (b) At 5.2 GHz. The structural parameters are $(H_L, L_L) = (4.5\text{ mm},\ 24.5\text{ mm})$, $(H_F, L_F) = (2.5\text{ mm},\ 10.5\text{ mm})$,

Typesetting math: 100%

$L_{FD} = 7.5$ mm, $(H_P, L_P) = (2.5 \text{ mm}, 9.0 \text{ mm})$, $(A_x, A_y) = (4.0 \text{ mm}, 3.0 \text{ mm})$, and $(L_x \times L_y) = (30 \text{ mm} \times 25.5 \text{ mm})$.

In the fourth step, a parasitic L element is added to the structure discussed in the third step, as shown in Fig. 1(a). The height of the parasitic L element is chosen to be equal to that of the inverted F element, as described in Section II: $H_P = H_F = 2.5$ mm. Fig. 3 shows the VSWR as a function of frequency for three values of the horizontal length of the parasitic L element, L_P, where the structural parameters for the inverted L and F elements are held at the values used in the third step: $(H_L, L'_L) = (4.5 \text{ mm}, 27.5 \text{ mm})$, $(H_F, L'_F) = (2.5 \text{ mm}, 11 \text{ mm})$, and $L_{FD} = 7.5$ mm. It is found that the parasitic L element generates resonances between 6 and 7 GHz. Note that the total length of the parasitic L, $H_P + L_P$, is close to one-quarter wavelength at the frequency where the minimum VSWR for each L_P appears: $H_P + L_P = 0.238\lambda_{6.8}$ at 6.8 GHz for $L_P = 8$ mm, $H_P + L_P = 0.253\lambda_{6.6}$ at 6.6 GHz for $L_P = 9$ mm, and $H_P + L_P = 0.267\lambda_{6.4}$ at 6.4 GHz for $L_P = 10$ mm, where λ_f is the wavelength at frequency f.

At this point there are two issues: 1) the VSWR curve is slightly shifted downward with respect to frequencies $f_{2.45}$ and $f_{5.2}$; and 2) the VSWR around $f_{5.2}$ is still larger than 2. These issues are solved by the following structural modifications: 1) reduction of the original horizontal strip line lengths L'_L and L'_F, and 2) widening of the strip width of the parasitic L element. Note that the widening of the strip width is realized by making a protrusion on the parasitic L element, where part of the strip line is widened to $w + A_y$ over length A_x, as shown in Fig. 1(b).

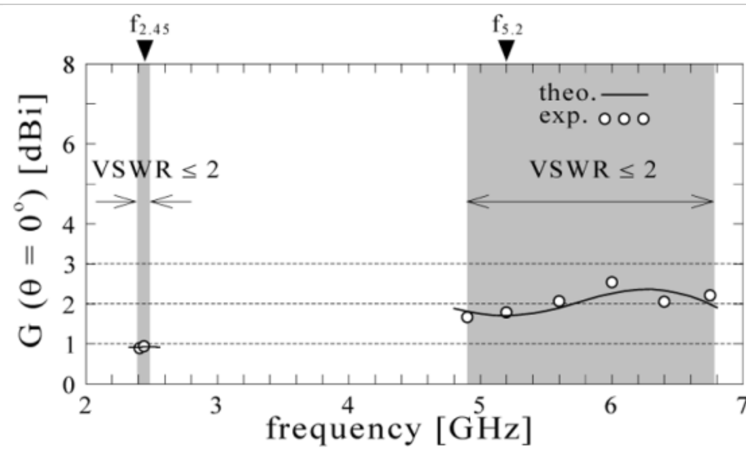

Fig. 6. Gain in the z-direction of an inverted FL antenna. The structural parameters are $(H_L, L_L) = (4.5 \text{ mm}, 24.5 \text{ mm})$, $(H_F, L_F) = (2.5 \text{ mm}, 10.5 \text{ mm})$, $L_{FD} = 7.5$ mm, $(H_P, L_P) = (2.5 \text{ mm}, 9.0 \text{ mm})$, $(A_x, A_y) = (4.0 \text{ mm}, 3.0 \text{ mm})$, and $(L_x \times L_y) = (30 \text{ mm} \times 25.5 \text{ mm})$.

The fifth step is to perform the aforementioned structural modifications for dual-frequency operation at 2.45 and 5.2 GHz. Using trial and error, the structural parameters are determined to be $(L_L, L_F, L_P) = (24.5 \text{ mm}, 10.5 \text{ mm}, 9.0 \text{ mm})$, $(A_x, A_y) = (4.0 \text{ mm}, 3.0 \text{ mm})$, and $L_{FD} = 7.5$ mm. Note that the horizontal lengths L_L and L_F are slightly smaller than the original lengths L'_L and L'_F in Fig. 1(a), respectively. Also note that the largest antenna height $(H_P + A_y)$ is very small with respect to the wavelength: $5.5 \text{ mm} = 0.045$ wavelength at 2.45 GHz. Fig. 4 shows the frequency response of the VSWR for the InvFLA defined with these final values for the structural parameters. This figure clearly indicates dual-frequency operation at $f_{2.45}$ and $f_{5.2}$. The frequency bandwidth for a $\text{VSWR} = 2$ criterion is 4.1% for the $f_{2.45}$ band and 31.8% for the $f_{5.2}$ band. The results are confirmed by the experimental results (white dots).

Fig. 5 shows the radiation patterns at $f_{2.45}$ and $f_{5.2}$. For confirmation of the FDTDM results, experimental results in the principal planes (x-z and y-z planes) are presented. Additionally, only the FDTDM results of the radiation patterns in the x-y plane at $f_{2.45}$ and $f_{5.2}$ are presented for completeness. The radiation patterns are useful in understanding the gain characteristic in the z direction $G(\theta = 0^\circ)$, which is shown in Fig. 6 together with experimental results, where the shadowed areas in the figure show the VSWR bands. It

Typesetting math: 100%

is found that the gain (with respect to an isotropic source) is approximately 0.9 dBi at $f_{2.45}$ and approximately 1.7 dBi at $f_{5.2}$, with a small gain variation in each VSWR band. These gain values are small due to the fact that the radiation is not highly directive, as seen from the radiation pattern E_{ϕ}.

The difference between the gains at $f_{2.45}$ and $f_{5.2}$ (i.e., the gain in the z-direction at 2.45 GHz is smaller than that at 5.2 GHz) is attributed to the following facts: 1) the radiation pattern E_{ϕ} at 2.45 GHz in each of the x-z and y-z planes is more omnidirectional than that at 5.2 GHz and 2) the radiation pattern E_{θ} at 2.45 GHz in each of the x-z and y-z planes (having a figure-eight pattern) shows a wider half-power beam width than that at 5.2 GHz.

An omnidirectional pattern is desirable for communications between a fixed base station antenna and an antenna installed in a *mobile* device. Note that, if a more omnidirectional E_{ϕ} pattern (in the x-z plane) is required for the InvFLA at 5.2 GHz, this can be achieved by placing the parasitic L element just under the horizontal strip line of the inverted F [13].

SECTION IV.
Conclusion

An InvFLA, made of a thin conducting film, has a card-type structure, where the radiation element is a compound of inverted L and F elements, which is adjacent to a co-planar ground plate. The design procedure for dual-frequency operation at $f = 2.45$ GHz and 5.2 GHz is described in five steps. In the first step, an inverted L element is designed for operation at 2.45 GHz. In the second step, an inverted F is designed for operation at 5.2 GHz. Based on these designs, a compound of the inverted L and F elements is investigated in the third step. Fine adjustment for dual-frequency operation is performed by introducing a parasitic L element in the fourth step and then modifying the parasitic L element in the fifth step.

It is found that the VSWR frequency bandwidth of the InvFLA is 4.1% around 2.45 GHz and 31.8% around 5.2 GHz. It is also revealed that the E_{ϕ} component of the radiation field from the InvFLA spreads out in a somewhat omnidirectional fashion. Further analysis shows that the gain variation in each VSWR band is small. The gain in the z direction (normal to the antenna plane) is 0.9 dBi at 2.45 GHz and 1.7 dBi at 5.2 GHz.

ACKNOWLEDGMENT

The authors would like to thank V. Shkawrytko for his invaluable help in the preparation of this manuscript.

Authors

Figures

References

Citations

Keywords

Metrics

EXHIBIT C

Compact Planar Monopole Antenna for Multi-band Mobile Phones

Xu Jing, Zhengwei Du and Ke Gong
State Key Lab on Microwave and Digital Communications
Department of Electronic Engineering
Tsinghua University, Beijing, People's Republic of China
E-mail: jingxu99@mails.tsinghua.edu.cn

***Abstract* - A novel planar monopole antenna suitable for mobile handset applications is presented in this paper. The antenna is mainly composed of a rectangular radiating patch with a meandered slot on, and due to the slot three branches are constructed, two resonating branches and a tuning one. The antenna is printed on a FR4 substrate and fed by a 50Ω microstrip line. A prototype has been fabricated and studied. The resulting antenna is able to operate in the GSM, DCS, PCS, UMTS and WLAN bands with a voltage standing wave radio (VSWR) better than 2.5. Both simulated and measured results are presented.**

I. INTRODUCTION

The rapid development of modern wireless communication systems has caused wide interests in designing wide-band and multi-band antennas. A variety of antenna configurations have been reported to be promising candidates for mobile handsets, such as the planar inverted-F antenna (PIFA)[1]-[3], the planar wire antenna[4], and the planar monopole antenna[5]-[8]. PIFA usually has a compact size, but its bandwidth is relatively narrow and a sufficient height from the ground plane has to be kept to achieve the acceptable performances. The planar wire antenna exhibits a much wider bandwidth, but its large size and external configuration make it less practicable in mobile applications. The planar monopole antennas proposed in [5]-[8] generally possess compact size, sufficient bandwidth and satisfying radiation patterns. However, their structures are all 3-dimensional instead of 2-dimensional, increasing the manufacture difficulty and cost.

In this paper, a novel planar monopole antenna with a 2-dimensional structure is introduced. Both the structure and the parameters are carefully adjusted to achieve multi-resonances, sufficient bandwidths and convenient profile. Printed on a dielectric board, the antenna consists of three branches. At first, two branches are designed to resonate at certain frequencies, and then another one is added for fine tuning. With a small area of $36 \times 15\ mm^2$, the antenna meets the demand of the following communication standards: GSM (Global System for Mobile communications, 890-960 MHz), DCS (Digital Communication System, 1710-1880 MHz), PCS (Personal Communication Services, 1850-1990 MHz), UMTS (Universal Mobile Telecommunications System, 1920-2170 MHz), and WLAN (Wireless Local Area Network, 2400-2484 MHz). Details of the design are described in the second section, and measured results of the prototype in the third.

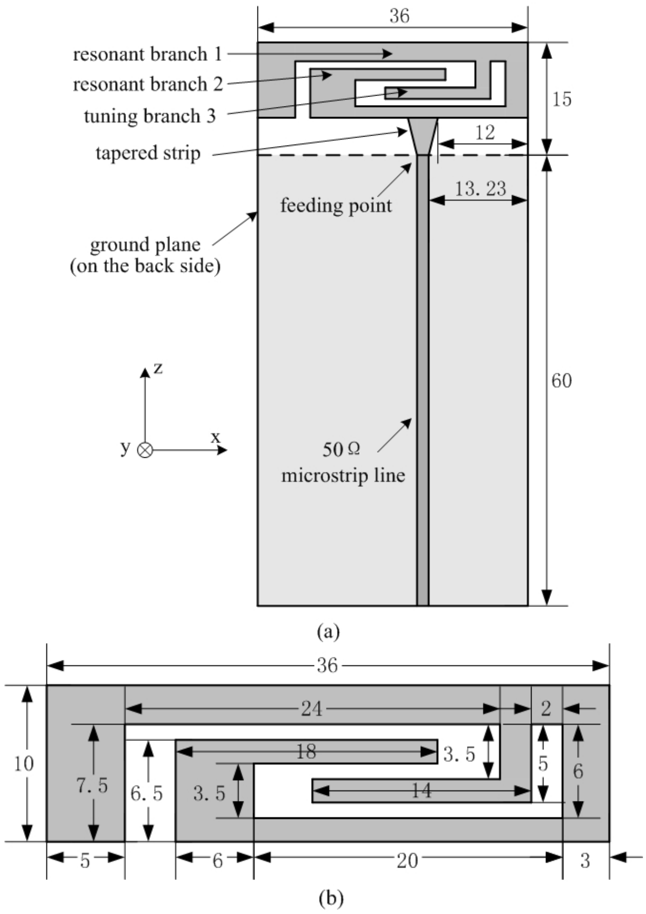

Fig. 1. Configuration of the proposed planar monopole antenna. (a) General view of the antenna. (b) Detailed dimensions of the main radiating element. All dimensions are in millimeter.

II. Antenna Design

The general view of the proposed antenna is shown in Fig. 1(a), and details of the design dimensions in Fig. 1(b). The planar monopole occupies an area of 36×15 mm^2, and is printed on a 0.8-mm FR4 substrate (relative permittivity 4.4). The substrate, 36 mm in width and 75 mm in length, is considered to be the typical system circuit board of a mobile phone. On the back surface of the substrate, a ground plane of 36 mm in width and 60 mm in length is printed and treated as the system ground plane. The monopole is fed by a 50Ω microstrip line, as shown in Fig. 1(a).

The main radiating element is in the shape of a rectangle. With a meandered slot on the patch, three branches are constructed, which are designated as resonant branch 1 (the longer branch), resonant branch 2 (the shorter branch) and tuning branch 3 (the additional inner branch) respectively in Fig. 1. Between the rectangular patch and the feeding microstrip line, a tapered strip of 5-mm length is printed. The width of the strip changes linearly from 1.54 mm at the feeding point to 4 mm at the edge of the patch, improving the impedance matching at the feeding point.

At the beginning of the design, only the two resonant branches 1 and 2 are taken into account, which present two surface current paths of different lengths. The length of the longer path, calculated from the feeding point to the open end of resonant branch 1, is selected to be about 75 mm. This value is very close to one-quarter wavelength of 900-MHz frequency in free space. It is instructive to note that the resonating frequency is affected by both the length of the path and the width of the open end. In the same way, the length of the shorter path, from the feeding point to the open end of resonant branch 2, is found to be about 35 mm, approximately one-quarter wavelength of 2-GHz frequency. The slight difference is mainly because of the existence of the substrate, which shortens the resonating wavelength.

The antenna with only the two resonant branches 1 and 2 is capable of dual-band operation. However, the bandwidth is not sufficient to cover all the five bands listed above, especially the WLAN band. Thus, the tuning branch 3 is added at a proper position on resonant branch 1. Simulation results have shown that by carefully adjusting the dimensions of branch 3, the fundamental and higher modes of branch 1 can be tuned to appropriate frequencies. According to the simulation data, the resonant frequency of the fundamental mode is reduced from 960 MHz to 910 MHz. As for the higher mode, the resonant frequency is changed from higher than 3 GHz to about 2.5GHz. Thus, the antenna with all the three branches is suitable for GSM/DCS/PCS/UMTS/WLAN operation. The simulated return loss of the antennas with and without tuning branch 3 is presented in Fig. 2 for reference. The results are gained through Ansoft HFSS (High Frequency Structure Simulator) software.

III. Measured Results

A prototype was constructed according to the design dimensions, and the measured return loss is shown in Fig. 3.

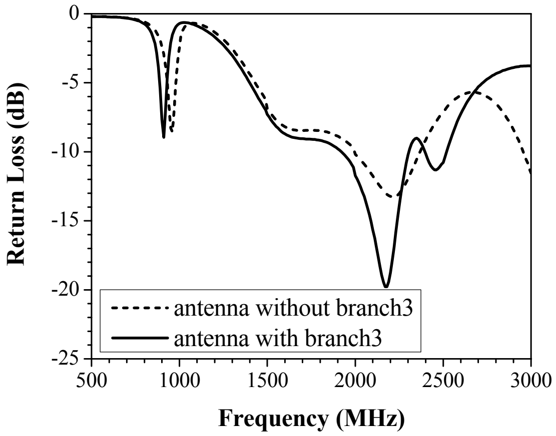

Fig. 2. Simulated return loss of the antennas with and without tuning branch 3.

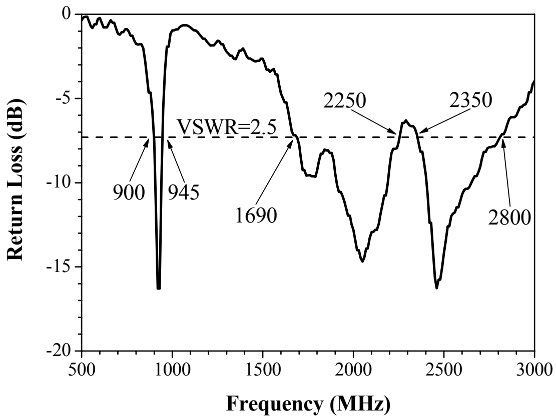

Fig. 3. Measured return loss of the proposed antenna.

Three resonating modes at 920, 2050 and 2460 MHz can be clearly observed. The first impedance bandwidth at 920 MHz is 45 MHz (900-945 MHz) with the VSWR (voltage standing wave ratio) better than 2.5. The second bandwidth at 2050 MHz is 560MHz (1690-2250 MHz), covering the DCS (1710-1880 MHz), PCS (1850-1990 MHz) and UMTS (1920-2170 MHz) bands. The third bandwidth at 2460 MHz is 450 MHz (2350-2800 MHz), covering the WLAN (2400-2484 MHz) band. However, it is observed that the bandwidth of the lowest resonating mode is insufficient to cover the GSM (890-960 MHz) band. More work has to be done to enhance the bandwidth, concentrating on the dimensions of resonant branch 1, the position of the feeding point, and the effects of parasitic elements.

Besides the return loss, the radiation characteristics of the proposed antenna are also studied. The measured radiation patterns in the x-y plane and y-z plane at 920 MHz, 1800 MHz, 2000 MHz and 2400 MHz are depicted in Fig.4. A lack

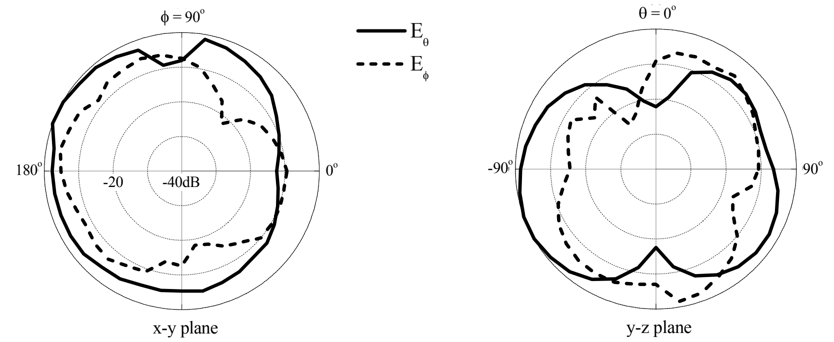

(a) 920 MHz

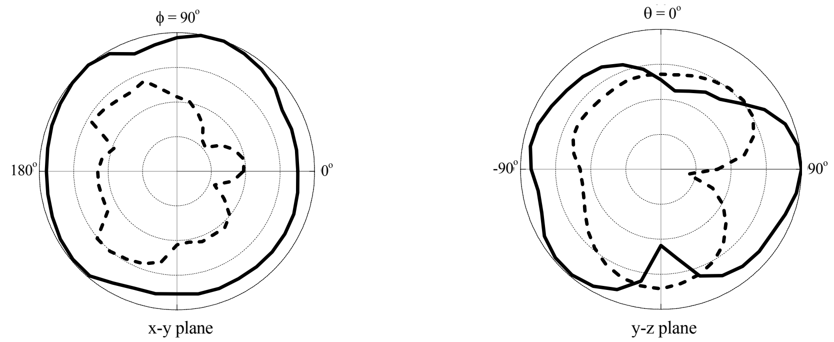

(b) 1800 MHz

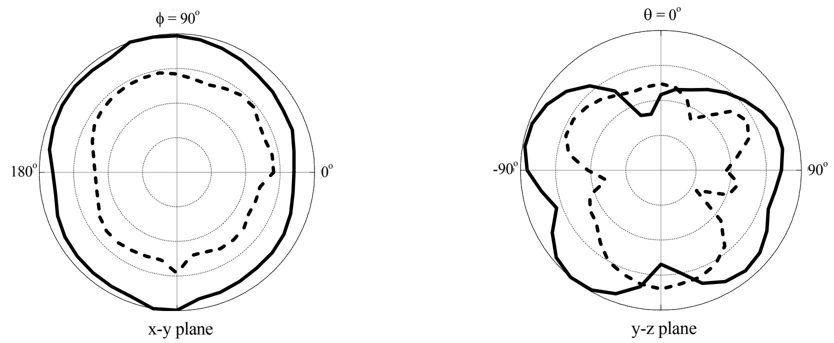

(c) 2000 MHz

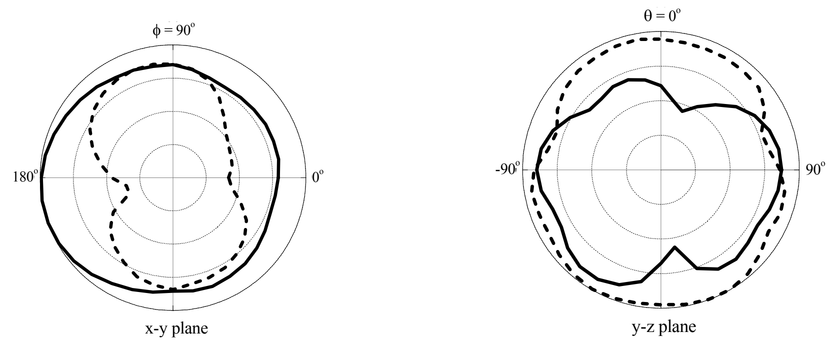

(d) 2400 MHz

Fig. 4. Measured radiation patterns of the proposed antenna at (a) 920 MHz, (b) 1800 MHz, (c) 2000 MHz and (d) 2400 MHz.

of polarization purity is observed in the figure. As a matter of fact, this is not a drawback since the urban communication environments are so complicated that both vertical and horizontal polarization may exist [9].

IV. CONCLUSIONS

A compact multi-band planar monopole antenna capable of mobile handset applications is proposed in the paper. A prototype is constructed based on the design. Occupying a small area of $36\times15\ mm^2$, the antenna meets the demand of GSM/DCS/PCS/UMTS/WLAN multi-band operation. Good radiation characteristics have been observed. The bandwidth for GSM band is still 25 MHz insufficient, more bandwidth-enhancement work being expected.

ACKNOWLEDGMENT

This work has been supported by the National Natural Science Foundation of China under Grants 60271007 and the Chinese National High-Tech program (863-2003AA123110). The authors appreciate the help in antenna measurement from G. Yan and F. Wang, Department of Electronic Engineering, Tsinghua University.

REFERENCES

[1] Pey-Ling Teng, Shyh-Tirng Fang, and Kin-Lu Wong, "PIFA with a bent, meandered radiating arm for GSM/DCS dual-band operation". *Antennas and Propagation Society Int. Symp.*, Vol.3, pp.107-110, Jun. 2003.

[2] Shih-Huang Yeh, Kin-Lu Wong, Tzung-Wern Chiou, and Shyh-Tirng Fang, "Dual-band planar inverted F antenna for GSM/DCS mobile phones". *IEEE Trans. Antennas Propagat.*, Vol.51, pp.1124-1126, May. 2003.

[3] P. Ciais, R. Staraj, G. Kossiavas, and C. Luxey, "Compact internal multiband antenna for mobile phone and WLAN standards". *Electron. Lett.*, Vol.40, Jul. 2004.

[4] R. L. Li, G. DeJean, M. M. Tentzeris, and J. Laskar, "Novel multi-band broadband planar wire antennas for wireless communication handheld terminals". *Antennas and Propagation Society Int. Symp.*, Vol.3, pp.44-47, Jun. 2003.

[5] Ching-Yuan Chiu, Pey-Ling Teng and Kin-Lu Wong, "Shorted, folded planar monopole antenna for dual-band mobile phone". *Electron. Lett.*, Vol.39, Sep. 2003.

[6] Pey-Ling Teng, Hong-Twu Chen, and Kin-Lu Wong, "Multi-frequency planar monopole antenna for GSM/DCS/PCS/WLAN operation". *Microwave Opt. Technol. Lett.*, Vol.36, pp.350-352, Mar. 2003.

[7] Pey-Ling Teng and Kin-Lu Wong, "Planar monopole folded into a compact structure for very-low-profile multiband mobile-phone antenna". *Microwave Opt. Technol. Lett.*, Vol.33, pp.22-25, Apr. 2002.

[8] I. F. Chen and C. M. Chiang, "Multi-folded tapered monopole antenna for wideband mobile handset applications". *Electron. Lett.*, Vol.40, May. 2004.

[9] P. Ciais, R. Staraj, G. Kossiavas, and C. Luxey, "Design of an internal quad-band antenna for mobile phones". *IEEE Microwave Wireless Comp. Lett.*, Vol.14, pp.148-150, Apr. 2004.

EXHIBIT C
ABSTRACT

Compact planar monopole antenna for multi-band mobile phones

Xu Jing ; Zhengwei Du ; Ke Gong All Authors

Abstract:
A novel planar monopole antenna suitable for mobile handset applications is presented in this paper. The antenna is mainly composed of a rectangular radiating patch with a meandered slot on, and due to the slot three branches are constructed, two resonating branches and a tuning one. The antenna is printed on an FR4 substrate and fed by a 50/spl Omega/ microstrip line. A prototype has been fabricated and studied. The resulting antenna is able to operate in the GSM, DCS, PCS, UMTS and WLAN bands with a voltage standing wave ratio (VSWR) better than 2.5. Both simulated and measured results are presented.

Published in: 2005 Asia-Pacific Microwave Conference Proceedings

Date of Conference: 04-07 December 2005

DOI: 10.1109/APMC.2005.1606884

Date Added to IEEE *Xplore*: 20 March 2006

Publisher: IEEE

Print ISBN:0-7803-9433-X

Conference Location: Suzhou

ISSN Information:

SECTION I.
Introduction

The rapid development of modern wireless communication systems has caused wide interests in designing wide-band and multi-band antennas. A variety of antenna configurations have been reported to be promising candidates for mobile handsets, such as the planar inverted-F antenna (PIFA) [1]– [3], the planar wire antenna [4], and the planar monopole antenna [5]– [8]. PIFA usually has a compact size, but its bandwidth is relatively narrow and a sufficient height from the ground plane has to be kept to achieve the acceptable performances. The planar wire antenna exhibits a much wider bandwidth, but its large size and external configuration make it less practicable in mobile applications. The planar monopole antennas proposed in [5]– [8] generally possess compact size, sufficient bandwidth and satisfying radiation patterns. However, their structures are all 3-dimensional instead of 2-dimensional, increasing the manufacture difficulty and cost.

In this paper, a novel planar monopole antenna with a 2-dimensional structure is introduced. Both the structure and the parameters are carefully adjusted to achieve multi-resonances, sufficient bandwidths and convenient profile. Printed on a dielectric board, the antenna consists of three branches. At first, two branches are designed to resonate at certain frequencies, and then another one is added for fine tuning. With a small area of $36 \times 15\ \mathrm{mm}^2$, the antenna meets the demand of the following communication standards: GSM (Global System for Mobile communications, 890–960 MHz), DCS (Digital Communication System, 1710–1880 MHz), PCS (Personal Communication Services, 1850–1990 MHz), UMTS (Universal Mobile Telecommunications System, 1920–2170 MHz), and WLAN (Wireless Local Area Network, 2400–2484 MHz). Details of the design are described in the second section, and measured results of the prototype in the third.

SECTION II.
Antenna Design

The general view of the proposed antenna is shown in Fig. 1(a), and details of the design dimensions in Fig. 1(b). The planar monopole occupies an area of $36 \times 15\ \mathrm{mm}^2$:, and is printed on a 0.8-mm FR4 substrate (relative permittivity 4.4). The substrate, 36 mm in width and 75 mm in length, is considered to be the typical system circuit board of a mobile phone. On the back surface of the substrate, a ground plane of 36 mm in width and 60 mm in length is printed and treated as the system ground plane. The monopole is fed by a 50Ω microstrip line, as shown in Fig. 1(a).

The main radiating element is in the shape of a rectangle. With a meandered slot on the patch, three branches are constructed, which are designated as resonant branch 1 (the longer branch), resonant branch 2 (the shorter branch) and tuning branch 3 (the additional inner branch) respectively in Fig. 1. Between the rectangular patch and the feeding microstrip line, a tapered strip of 5-mm length is printed. The width of the strip changes linearly from 1.54 mm at the feeding point to 4 mm at the edge of the patch, improving the impedance matching at the feeding point.

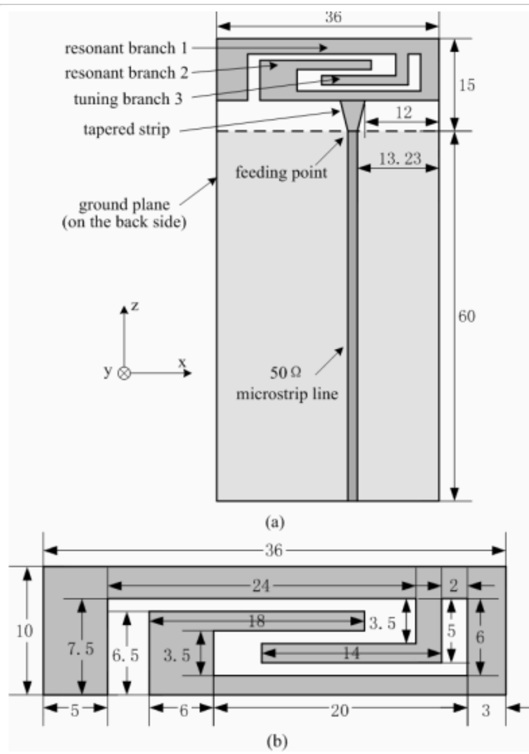

Fig. 1. Configuration of the proposed planar monopole antenna. (a) General view of the antenna. (b) Detailed dimensions of the main radiating element. All dimensions are in millimeter.

At the beginning of the design, only the two resonant branches 1 and 2 are taken into account, which present two surface current paths of different lengths. The length of the longer path, calculated from the feeding point to the open end of resonant branch 1, is selected to be about 75 mm. This value is very close to one-quarter wavelength of 900-MHz frequency in free space. It is instructive to note that the resonating frequency is affected by both the length of the path and the width of the open end. In the same way, the length of the shorter path, from the feeding point to the open end of resonant branch 2, is found to be about 35 mm, approximately one-quarter wavelength of 2-GHz frequency. The slight difference is mainly because of the existence of the substrate, which shortens the resonating wavelength.

he antenna with only the two resonant branches 1 and 2 is capable of dual-band operation. However, the bandwidth is not sufficient to cover all the five bands listed above, especially the WLAN band. Thus, the tuning branch 3 is added at a proper position on resonant branch 1. Simulation results have shown that by carefully adjusting the dimensions of branch 3, the fundamental and higher modes of branch 1 can be tuned to appropriate frequencies. According to the simulation data, the resonant frequency of the fundamental mode is reduced from 960 MHz to 910 MHz. As for the higher mode, the resonant frequency is changed from higher than 3 GHz to about 2.5GHz. Thus, the antenna with all the three branches is suitable for GSM/DCS/PCS/UMTS/WLAN operation. The simulated return loss of the antennas with and without tuning branch 3 is presented in Fig. 2 for reference. The results are gained through Ansoft HFSS (High Frequency Structure Simulator) software.

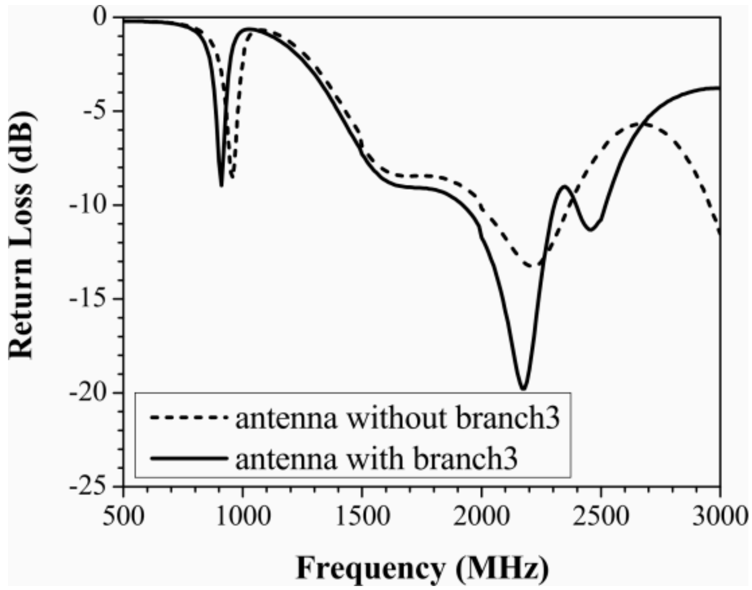

Fig. 2. Simulated return loss of the antennas with and without tuning branch 3.

SECTION III.
Measured Results

A prototype was constructed according to the design dimensions, and the measured return loss is shown in Fig. 3. Three resonating modes at 920, 2050 and 2460 MHz can be clearly observed. The first impedance bandwidth at 920 MHz is 45 MHz (900–945 MHz) with the VSWR (voltage standing wave ratio) better than 2.5. The second bandwidth at 2050 MHz is 560MHz (1690–2250 MHz), covering the DCS (1710–1880 MHz), PCS (1850–1990 MHz) and UMTS (1920–2170 MHz) bands. The third bandwidth at 2460 MHz is 450 MHz (2350–2800 MHz), covering the WLAN (2400–2484 MHz) band. However, it is observed that the bandwidth of the lowest resonating mode is insufficient to cover the GSM (890–960 MHz) band. More work has to be done to enhance the bandwidth, concentrating on the dimensions of resonant branch 1, the position of the feeding point, and the effects of parasitic elements.

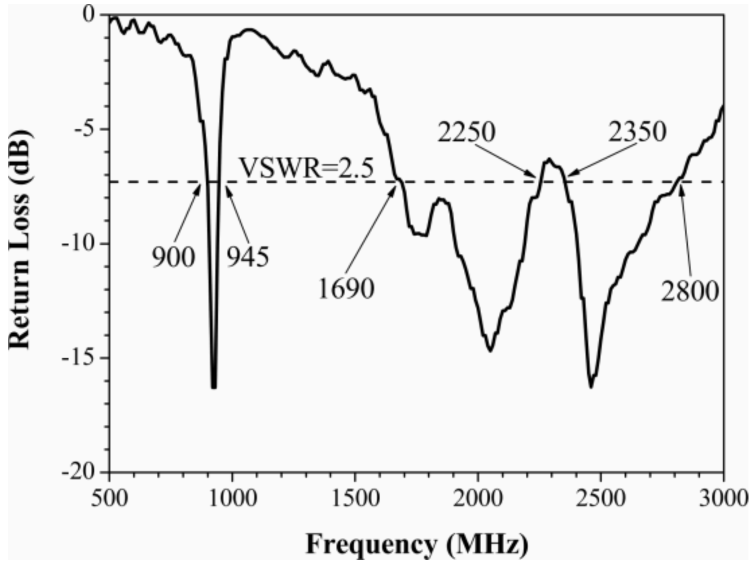

Fig. 3. Measured return loss of the proposed antenna.

Besides the return loss, the radiation characteristics of the proposed antenna are also studied. The measured radiation patterns in the x-y plane and y-z plane at 920 MHz, 1800 MHz, 2000 MHz and 2400 MHz are depicted in Fig. 4. A lack of polarization purity is observed in the figure. As a matter of fact, this is not a drawback since the urban communication environments are so complicated that both vertical and horizontal polarization may exist [9].

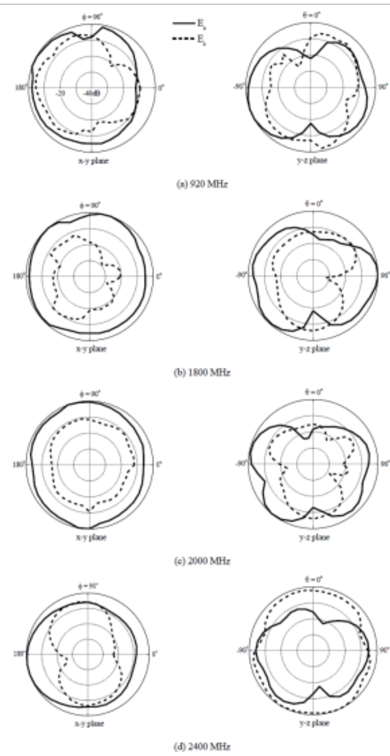

Fig. 4. Measured radiation patterns of the proposed antenna at (a) 920 MHz, (b) 1800 MHz, (c) 2000 MHz and (d) 2400 MHz.

Loading [MathJax]/extensions/MathZoom.js

SECTION IV.
Conclusions

A compact multi-band planar monopole antenna capable of mobile handset applications is proposed in the paper. A prototype is constructed based on the design. Occupying a small area of $36 \times 15\ mm^2$ the antenna meets the demand of GSM/DCS/PCSIUMTS/WLAN multi-band operation. Good radiation characteristics have been observed. The bandwidth for GSM band is still 25 MHz insufficient, more bandwidth-enhancement work being expected.

ACKNOWLEDGMENT

This work has been supported by the National Natural Science Foundation of China under Grants 60271007 and the Chinese National High-Tech program (863-2003AAI23110). The authors appreciate the help in antenna measurement from G. Yan and F. Wang, Department of Electronic Engineering, Tsinghua University.